bioRxiv preprint doi: https://doi.org/10.1101/583658; this version posted March 21, 2019. The copyright holder for this preprint (which was not certified by peer review) is the author/funder, who has granted bioRxiv a license to display the preprint in perpetuity. It is made available under aCC-BY-NC-ND 4.0 International license.

Novel cholinesterase paralogs of *Schistosoma mansoni* have perceived roles in cholinergic signaling, glucose scavenging and drug detoxification and are essential for parasite survival

Bemnet Tedla[1], Javier Sotillo[1,2], Darren Pickering[1], Ramon M. Eichenberger[1,3], Luke Becker[1], Alex Loukas[1] and Mark S. Pearson[1#].

[1]Centre for Molecular Therapeutics, Australian Institute of Tropical Health and Medicine, James Cook University, Cairns, Queensland, 4878, Australia.

[2]Centro Nacional de Microbiología, Instituto de Salud Carlos III, Majadahonda, Madrid, Spain.

[3]Institute of Parasitology, University of Zurich, Zurich, Switzerland

#Corresponding author

Dr Mark Pearson (mark.pearson@jcu.edu.au)

bioRxiv preprint doi: https://doi.org/10.1101/583658; this version posted March 21, 2019. The copyright holder for this preprint (which was not certified by peer review) is the author/funder, who has granted bioRxiv a license to display the preprint in perpetuity. It is made available under aCC-BY-NC-ND 4.0 International license.

Abstract

Cholinesterase (ChE) function in schistosomes is essential for orchestration of parasite neurotransmission but has been poorly defined with respect to the molecules responsible. Interrogation of the *S. mansoni* genome has revealed the presence of three ChE domain-containing genes (*Smche*)s, which we have shown to encode two functional acetylcholinesterases (AChE)s (*Smache1* – smp_154600 and *Smache3* – smp_136690) and a butyrylcholinesterase (BChE) (*Smbche1* – smp_125350). Antibodies to recombinant forms of each *Sm*ChE localized the proteins to the tegument and neuromusculature of adults and schistosomula and developmental expression profiling differed among the three molecules, suggestive of functions extending beyond traditional cholinergic signaling. For the first time in schistosomes, we identified ChE enzymatic activity in fluke excretory/secretory (ES) products and, using proteomic approaches, attributed this activity to the presence of *Sm*AChE1 and *Sm*BChE1. To address the hypothesis that tegumental AChE mediates exogenous glucose scavenging by the parasite, we show that RNAi-mediated knockdown of *smache1* and *smache3*, but not *smbche1*, significantly reduces glucose uptake by schistosomes. Parasite survival *in vitro* and *in vivo* was significantly impaired by silencing of each *smche*, either individually or in combination, attesting to the essential roles of these molecules. Lastly, in the first characterization study of a BChE from helminths, evidence is provided that *Sm*BChE1 may act as a bio-scavenger of AChE inhibitors as the addition of recombinant *Sm*BChE1 to parasite cultures mitigated the effect of the anti-schistosome AChE inhibitor DDVP (DDVP), whereas *smbche1*-silenced parasites displayed increased sensitivity to DDVP.

bioRxiv preprint doi: https://doi.org/10.1101/583658; this version posted March 21, 2019. The copyright holder for this preprint (which was not certified by peer review) is the author/funder, who has granted bioRxiv a license to display the preprint in perpetuity. It is made available under aCC-BY-NC-ND 4.0 International license.

Author summary

Cholinesterases - aceytlcholinesterases (AChE)s and butyrylcholinesterases (BChE)s - are multi-functional enzymes that play a pivotal role in the nervous system of parasites by regulating neurotransmission through acetylcholine hydrolysis. Herein, we provide a detailed characterization of schistosome cholinesterases using molecular, enzymatic and gene-silencing approaches and show evidence for these molecules having roles in glucose scavenging and drug detoxification, in addition to their neuronal function. Further, we demonstrate the importance of these proteins to parasite development and survival through gene knockdown experiments in laboratory animals, providing evidence for the use of these proteins in the development of novel intervention strategies against schistosomiasis.

Introduction

The functioning of the nervous system is a tightly regulated process controlled through multiple catalytic and non-catalytic signaling proteins. Among the catalytic molecules, cholinesterases (ChEs) play a pivotal role in regulating the signaling activity of the nervous system. There are two major types of ChEs, acetylcholinesterase (AChE) and pseudocholinesterase, or butyrylcholinesterase (BChE), and they can be distinguished both kinetically and pharmacologically [1]. AChE selectively hydrolyzes the neurotransmitter acetylcholine (ACh) to maintain neurotransmitter homeostasis [2] while the main role of BChE is widely accepted to be the detoxification of organophosphorus esters which are inhibitors of AChE [3]. ChEs are generally believed to be functionally redundant in cholinergic signaling with the main differences between paralogs lying in their spatial and temporal expression as well as non-cholinergic functionality [4, 5].

bioRxiv preprint doi: https://doi.org/10.1101/583658; this version posted March 21, 2019. The copyright holder for this preprint (which was not certified by peer review) is the author/funder, who has granted bioRxiv a license to display the preprint in perpetuity. It is made available under aCC-BY-NC-ND 4.0 International license.

The nervous system of helminths has long been a potential target for therapeutic agents as it plays several crucial roles in parasite biology that are fundamental to survival, including coordinating motility within and outside of the host, feeding and reproduction [6-10]. The *Schistosoma* nervous system is particularly important in this respect as this parasite lacks a body cavity and circulating body fluid [11, 12] and, as a result, its signaling functions are chiefly achieved via neurotransmission. The primary neurotransmitter that schistosomes utilize is acetylcholine (ACh), which allows muscle contraction. The physiological concentration of ACh, however, must be maintained otherwise it triggers paralysis and this is achieved primarily through the action of AChE [6-8].

While AChE activity has been documented extensively in *S. mansoni* (reviewed in [13]), most of the work has involved studies on parasite extracts or native *Sm*ChE purified by inhibitor-affinity chromatography, making it difficult to attribute function to any one particular *Sm*ChE molecule. Further, more recent, but still "pre-genomic", studies have documented only one AChE-encoding gene in *S. mansoni* and other species [14, 15]. In 2016, You *et al.* characterized AChE activity in *S. japonicum* extracts and at a molecular level, but only through the expression of one recombinant AChE [16]. Moreover, to the best of our knowledge, genes encoding proteins with BChE activity have not been previously described in schistosomes or any other helminth. Interrogation of the now fully annotated *S. mansoni* genome [17] has revealed three different *Sm*ChE paralogs; however, their individual contributions to ChE function remain unknown.

Traditionally, ChEs have been regarded solely as neurotransmitter terminators; however, there is increasing data to suggest that these enzymes play a variety of roles that extend beyond this cholinergic function due to their presence in multiple cell types and subcellular locations [4, 5,

bioRxiv preprint doi: https://doi.org/10.1101/583658; this version posted March 21, 2019. The copyright holder for this preprint (which was not certified by peer review) is the author/funder, who has granted bioRxiv a license to display the preprint in perpetuity. It is made available under aCC-BY-NC-ND 4.0 International license.

18, 19]. In schistosomes, AChE has been localized to the tegument as well as the neuromusculature [16, 20, 21] and a proposed function for tegumental AChE has been mediation of glucose uptake by the parasite from the external environment [22]. The exact mechanism for this process is still unclear but the proposed initiating step is by limiting the interaction of host ACh with tegumental nicotinic ACh receptors (nAChRs), a hypothesis bolstered by the observation that glucose uptake is ablated by the use of membrane-impermeable AChE and nAChR inhibitors in *S. mansoni* [22, 23] and RNAi-mediated AChE silencing in *S. japonicum* [24]. The nAChRs are also associated both spatially and temporally with surface AChE expression and are concentrated on the tegument [25], the major site of glucose uptake [26].

Many intestinal nematodes secrete AChE [27-30], which, where studied, orchestrate exogenous cholinergic activities. It has also been indirectly shown that the nematode *N. brasiliensis* employs parasite-derived AChE to alter the host cytokine environment to inhibit M2 macrophage recruitment, a condition favorable to worm survival [31]. Despite this breadth of literature in nematodes, there has been no documentation of secreted AChE activity from schistosomes.

Herein we describe and functionally characterize using gene silencing and enzymatic approaches, a novel AChE and BChE from *S. mansoni* and further characterize the only previously identified AChE-encoding gene from the parasite. Importantly, we show through gene knockdown that each *smche* is essential to *S. mansoni* development and survival, highlighting them as targets for novel anti-schistosomal intervention strategies.

bioRxiv preprint doi: https://doi.org/10.1101/583658; this version posted March 21, 2019. The copyright holder for this preprint (which was not certified by peer review) is the author/funder, who has granted bioRxiv a license to display the preprint in perpetuity. It is made available under aCC-BY-NC-ND 4.0 International license.

Results

Identification of novel genes encoding ChE proteins in S. mansoni

Three putative ChE paralogs were identified from interrogation of the *S. mansoni* genome: *smache1* (Smp_154600), *smbche1* (Smp_125350) and *smache3* (Smp_136690). The predicted *Sm*ChEs were then aligned with characterized AChE enzymes from *Homo sapiens*, the electric eel *Torpedo californica*, and the nematode *Caenorhabditis elegans* (Figure 1). Homology analysis of amino acid sequences revealed that *Sm*AChE1, *Sm*BChE1, and *Sm*AChE3 share (32-35%) sequence identity and (49-52%) sequence similarity. Further, all *Sm*ChEs have 36-40% amino acid identity with *H. sapiens* and *T. californica* AChE. All identified *Sm*ChEs had ChE-specific characteristics, including a catalytic triad with an active site serine, which is required for ester hydrolysis [32]. Interestingly, the His residue of the catalytic triad of *Sm*BChE1 appears to have been substituted for Gln, a change consistent among all the BChE1 homologs shown for other Platyhelminthes, but not nematode or model organism BChE1 sequences (Figure S1). A 3D model of the three *Sm*ChEs was constructed by homology modeling with AChE from model organisms (*H. sapiens* and *T. californica* (Figure S2). All three *Sm*ChEs exhibited predicted folding characteristics of the functional globular enzymes as most of the α-helical and β-stranded sheets were tightly aligned. Each predicted *Sm*ChE structure consisted of a ChE catalytic domain but, although the core architecture of the catalytic gorges was well aligned, regions that are associated with substrate specificity and catalytic efficiency were disparate. In particular, and in agreement with the sequence alignment, the catalytic triad of *Sm*BChE1 was predicted to be Ser-Gln-Glu instead of the canonical Ser-His-Glu present in the other two paralogs. A phylogenetic tree of the alignment (Figure S3) shows that *Sm*ChEs were clustered into three distinct branches, with *Sm*ChE1 being phylogenetically distinct from *Sm*BChE1 and *Sm*AChE3. In addition, each *Sm*ChE was grouped together with closely related flatworms, including other *Schistosoma* species.

bioRxiv preprint doi: https://doi.org/10.1101/583658; this version posted March 21, 2019. The copyright holder for this preprint (which was not certified by peer review) is the author/funder, who has granted bioRxiv a license to display the preprint in perpetuity. It is made available under aCC-BY-NC-ND 4.0 International license.

147 Importantly, as shown in the sequence alignment, *Sm*ChEs are divergent from the human
148 homolog. Reflective of the catalytic triad residue difference (Figure S1), trematode BChEs are
149 phylogenetically divergent from nematode and human BChEs (Figure S4).
150
151 ***Developmental expression analysis of SmChE genes***
152 Gene expression patterns of the three *Sm*ChE paralogs across different developmental stages
153 were measured using semi-quantitative qPCR (Figures 2A-C) and this data was used to
154 generate a comparative expression heat map of all three genes (Figure 2D). While all *smche*
155 developmental expression patterns were variable, the transcript levels of all three genes were
156 relatively lower in cercariae compared to the other developmental stages. Overall, the transcript
157 levels of *smache1* and *smache3* genes in most life stages were higher than that of *smbche1*. In
158 adult worms, *smache1* was expressed at higher levels, specifically in male parasites, followed
159 by sporocysts.
160
161 ***Immunolocalization of SmChEs***
162 To gain insight into the anatomical sites of expression of ChE proteins in S. *mansoni*, *Sm*ChEs
163 were immunolocalized in whole juvenile and sectioned adult parasites. In adults, and consistent
164 with their predicted cholinergic function, all *Sm*ChEs were expressed throughout the worms'
165 internal structures (presumably localizing to the neuromusculature) and on the tegument
166 surface. *Sm*AChE1 was the least uniformly distributed of all *Sm*ChEs, localizing mostly to
167 the tegument (Figure 3A). Additionally, anti-*Sm*ChE antibodies were able to detect
168 homologous ChEs in adult *S. haematobium* sections. *Sm*ChE proteins were detected in all
169 stages of larval development tested and, as was the case with adult worms, localized to the
170 tegument (Figure 3B).
171

bioRxiv preprint doi: https://doi.org/10.1101/583658; this version posted March 21, 2019. The copyright holder for this preprint (which was not certified by peer review) is the author/funder, who has granted bioRxiv a license to display the preprint in perpetuity. It is made available under aCC-BY-NC-ND 4.0 International license.

Expression and ChE activity of fSmChEs

Soluble, functionally active proteins were expressed in *P. pastoris*, purified via IMAC and tested for ChE activity. Both f*Sm*AChE1 and f*Sm*AChE3 demonstrated significantly stronger hydrolase activity when AcSCh was used as a substrate, compared to f*Sm*BChE1 and, conversely, f*Sm*BChE1 hydrolyzed BcSCh to significantly higher levels compared to f*Sm*AChE1 and f*Sm*AChE3 (Figure 4A). All paralogs exhibited Michaelis–Menten kinetics (Table 1) when hydrolyzing their designated substrate, with f*Sm*AChE1 having a substrate affinity approximately twice that of f*Sm*AChE3. In addition, preferred substrate activity of both f*Sm*AChE1 and f*Sm*AChE3 was inhibited by DDVP, an AChE inhibitor, whereas iso-OMPA, a specific inhibitor of BChE, only inhibited *Sm*BChE1 activity (Figure 4B).

Table 1. Kinetic parameters of f*Sm*ChEs

SmChE paralog	Vmax (nmol/min/mg)	Km (mM)
f*Sm*AChE1	5.57 ± 0.54*	5.83 ± 1.62*
f*Sm*AChE3	5.59 ± 1.37*	10.87 ± 6.17*
f*Sm*BChE1	1.7 ± 0.09#	34.38± 12.71#

*Hydrolysis of AcSCh.

#Hydrolysis of BcSCh.

BChE and secreted ChE activity in schistosomes

Although the presence of nonspecific ChE activity has long been known in schistosomes [33], the identity of the gene product and its function remain unknown. Prompted by the identification of *Sm*BChE1 as a BChE, based on its substrate preference and enzymatic inhibition by iso-OMPA, we sought to investigate the distribution of BChE activity in juvenile and adult schistosomes. Extracts from *S. mansoni* schistosomula had higher BChE activity compared to *S. mansoni* adult worms (Figure 5A), and that activity was significantly greater in

bioRxiv preprint doi: https://doi.org/10.1101/583658; this version posted March 21, 2019. The copyright holder for this preprint (which was not certified by peer review) is the author/funder, who has granted bioRxiv a license to display the preprint in perpetuity. It is made available under aCC-BY-NC-ND 4.0 International license.

194 *S. mansoni* compared with *S. haematobium* adults (Figure 5B). Varied amounts of AChE
195 activity were detected in ES from all developmental stages tested. ES products from adult males
196 had double the AChE activity of adult female ES products ($P < 0.001$), while cercariae ES
197 exhibited the highest activity (at least ten-fold more than male ES products ($P < 0.0001$)) and
198 egg ES had the lowest (Figure 5C). Availability of ES precluded the measurement of secreted
199 BChE activity from all developmental stages but, of those tested, activity in schistosomula ES
200 products was the highest - twice as high as that of adult ($P < 0.01$) and cercariae ($P < 0.01$) ES
201 (Figure 5D). *Sm*ChEs were purified from ES products of *S. mansoni* adult worms using
202 edrophonium–sepharose affinity chromatography. Purification resulted in an activity increase
203 of more than 200-fold relative to crude ES (Figure 5E). Resolution of the purified proteins by
204 SDS-PAGE resulted in a doublet with a major band migrating at 70 kDa under denaturing and
205 reducing conditions (Figure 5F). The identity of purified, secreted *Sm*ChEs was substantiated
206 by in-gel LC-MS/MS analysis with the peptide data generated used to interrogate the *S.*
207 *mansoni* proteome (predicted from the *S. mansoni* genome -
208 http://www.genedb.org/Homepage/Smansoni). The false discovery rate was set at <1% and
209 only proteins with at least two unique peptides having significant Mascot identification scores
210 ($P < 0.05$) were considered. The top protein hits were identified as *Sm*AChE1 (Smp_154600)
211 and *Sm*BChE1 (Smp_125350); *Sm*AChE1 had a relative abundance of more than 40-fold that
212 of *Sm*BChE1 (supplementary table 3).
213
214 ***RNAi-mediated smche transcript and SmChE protein reduction***
215 Schistosomula electroporated with *smache1* siRNA showed respective decreases in *Sm*AChE1
216 mRNA levels of 55.4% ($P \leq 0.05$) and 81.3% ($P \leq 0.001$) at one and seven days post-treatment,
217 respectively, compared to the *luc* control (Figure 6A), while treating parasites with *smbche1*
218 siRNA caused 32.0% ($P \leq 0.001$) and 84.5% ($P \leq 0.001$) suppression of *smbche1* mRNA

bioRxiv preprint doi: https://doi.org/10.1101/583658; this version posted March 21, 2019. The copyright holder for this preprint (which was not certified by peer review) is the author/funder, who has granted bioRxiv a license to display the preprint in perpetuity. It is made available under aCC-BY-NC-ND 4.0 International license.

219 expression at day 3 and 7 after electroporation, respectively, compared to the *luc* control
220 (Figure 6B). Treatment of schistosomula with *smache3* siRNA resulted in respective decreases
221 in *smache3* mRNA levels of 27.4% ($P \leq 0.001$) and 47.2% ($P \leq 0.01$) three and seven days
222 after electroporation, compared to the *luc* control (Figure 6C). Schistosomula electroporated
223 with a cocktail of all three *smche* siRNAs showed decreases of all three transcript levels over
224 time, with *smache3* mRNA levels decreasing by an average of 90% ($P \leq 0.001$) by day 3 after
225 treatment, compared to the *luc* control (Figure 6D).

226 Seven days after treatment with *Sm*AChE1, *Sm*BChE1 or *Sm*AChE3 siRNAs, schistosomula
227 showed decreases in *Sm*AChE1, *Sm*BChE1 or *Sm*AChE3 protein expression of 73%, 59% and
228 46%, respectively, compared to luciferase controls (Figure 6E).

229

230 ***Suppression of SmChE activity***

231 Suppression of AChE activity was seen in *smache1* and *smache3* siRNA-treated parasites from
232 5 and 3 days after electroporation, respectively (Figure 7A), compared to the *luc* control, while
233 schistosomula treated with *smbche1* siRNA did not show any significant reduction in BChE
234 activity, even 7 days after electroporation (Figure 7B). Parasites electroporated with a cocktail
235 of all three *smche* siRNAs showed significant decreases in AChE activity at 3 days (62%
236 reduction, $P \leq 0.001$), 5 days (67% reduction, $P \leq 0.001$) and 7 days (71% reduction, $P \leq 0.001$)
237 after treatment (Figure 7C). BChE activity was not measured in the cocktail siRNA treatment
238 group.

239 Individual silencing of *smache1* or *smache3* genes and combined silencing of all three *smche*
240 genes reduced glucose uptake in schistosomula by 24.9% ($P \leq 0.001$), 32.34% ($P \leq 0.001$) and
241 38.61% ($P \leq 0.001$) at 48 h post-treatment, respectively, relative to the *luc* control. However,
242 *smbche1*-silenced parasites showed no significant changes in glucose uptake at the same

bioRxiv preprint doi: https://doi.org/10.1101/583658; this version posted March 21, 2019. The copyright holder for this preprint (which was not certified by peer review) is the author/funder, who has granted bioRxiv a license to display the preprint in perpetuity. It is made available under aCC-BY-NC-ND 4.0 International license.

timepoint and there was no difference in the glucose consumed by the *smache1* or *smache3* siRNA-treated groups compared with the cocktail siRNA-treated group (Figure 7D). Transcript levels of the glucose transporters, *sgtp1* and *sgtp4*, were neither decreased nor significantly increased in individual or cocktail *smche*-silenced parasites (Figure S5).

Effects of smche silencing on schistosomula viability in vitro and development in vivo. Parasites treated with *smache1*, *smbche1* or *smache3* siRNAs showed significant decreases in viability at days 3, 5 and 1 after treatment, respectively, compared to *luc* controls. At days 5 and 7 post-treatment, the most significant decrease in parasite viability was seen in the group which received the cocktail siRNA treatment, compared to *luc* controls. Furthermore, viability in this group was also significantly lower than it was for any individual treatment at these two time points (Figure 8A).

To examine whether RNAi-mediated *smche* suppression reduced parasite viability *in vivo*, mice were infected with *smche*-silenced parasites and worm burdens were measured after three weeks. From two independent experiments, there was an average 88.15%, 55.15%, 75.95% and 88.35% decrease in adult fluke burdens from mice injected with *smache1*-, *smbche1*-, *smache3*- and *smche* cocktail-silenced schistosomula, respectively, compared to mice infected with *luc*-treated parasites (Figures 8B and C). All worm burden decreases were significant and there was no significant difference in fluke burdens between mice injected with *luc*-treated parasites and non-electroporated control parasites. All mice had been successfully infected with parasites, as serum from necropsied mice contained parasite-specific antibodies (data not shown). Compared to *luc*-treated parasites, worms recovered from *smche*-treated parasites showed no difference in *smche* transcript levels (data not shown).

bioRxiv preprint doi: https://doi.org/10.1101/583658; this version posted March 21, 2019. The copyright holder for this preprint (which was not certified by peer review) is the author/funder, who has granted bioRxiv a license to display the preprint in perpetuity. It is made available under aCC-BY-NC-ND 4.0 International license.

Bio-scavenging of carboxylic esters by SmBChE1

The hypothesis that *Sm*BChE may act as a molecular decoy in schistosomes and detoxify the effects of organophosphorus AChE inhibitors was examined by testing whether (a) inhibition of parasite-derived BChE potentiated the effects of DDVP (an organophosphorous AChE inhibitor) and (b) addition of exogenous BChE (f*Sm*BChE1) mitigated the effects of DDVP. DDVP activity in schistosome extracts significantly increased in the presence of increasing amounts of the BChE inhibitor, iso-OMPA (Figure 9A) and DDVP-mediated killing of schistosomula was significantly increased in the presence of iso-OMPA (60.9% compared with 21.8%; $P < 0.0001$) (Figure 9B). Further, *smbche1*-silenced schistosomula were significantly more susceptible to DDVP-mediated killing than *luc*-treated controls (83.44% compared with 22.95%; $P < 0.0001$) (Figure 9C). Conversely, DDVP-induced inhibition of AChE in extracts was completely ablated in the presence of f*Sm*BChE (Figure 9D) and schistosomula were increasingly resistant to DDVP-mediated killing with the addition of increasing amounts of recombinant protein to the culture media (Figure 9E).

Discussion

Cholinesterase (ChE) activity in *S. mansoni* was first described by Bueding in 1952 [33] and was well characterized biochemically in the four decades succeeding this discovery. The technological limitations of this time period meant that most of the evidence for *Sm*ChEs came from whole worm studies and analyses of crude parasite extracts (reviewed in [13]), which could not ascribe ChE activity to any particular protein. Several studies in the early 2000's characterized a single AChE from *S. mansoni* (Smp_154600 in the current gene annotation nomenclature) and its direct homolog in other species of schistosomes [14, 15, 21], but lack of a comprehensive schistosome genome annotation at the time precluded identification of more ChE family members. Interrogation of the most recent iteration of the *S. mansoni* genome

bioRxiv preprint doi: https://doi.org/10.1101/583658; this version posted March 21, 2019. The copyright holder for this preprint (which was not certified by peer review) is the author/funder, who has granted bioRxiv a license to display the preprint in perpetuity. It is made available under aCC-BY-NC-ND 4.0 International license.

292 assembly has identified two additional ChE-encoding genes that are paralogs to Smp_154600
293 (which we have termed *Sm*AChE1); Smp_125350 (*Sm*BChE1) and Smp_136690 (*Sm*AChE3).
294 In this current study, we have provided a more in-depth characterization of the previously
295 documented *Sm*AChE1 and described two novel ChEs from *S. mansoni*: *Sm*AChE3 – an AChE
296 not previously reported; and *Sm*BChE1 – a BChE which, to the best of our knowledge, has
297 never been documented in the helminth literature.
298
299 All *Sm*ChEs share a modest level of identity which is consistent with their divergence over
300 evolutionary time, an occurrence that is possibly due to a series of gene duplications due to the
301 phylogenetic distance between the relative clades. This divergence between *Sm*ChEs and, also,
302 ChEs of other organisms, provides evidence for the increasing reports of non-cholinergic
303 functions of ChEs in the literature. Additionally, the relative lack of sequence identity between
304 SmChEs and human ChEs suggests potential scope for the development of intervention
305 strategies targeting schistosome ChEs that will not affect the host. Despite the diversity
306 between ChEs, all enzymes analyzed herein would appear to be enzymatically active as they
307 possessed a catalytic triad with an active site serine, the amino acid responsible for ester
308 hydrolysis [32]. It is interesting to note, however, the catalytic triad His – Gln substitution in
309 *Sm*BChE1 (and the other platyhelminth BChE1 homologs); while this change is not a hallmark
310 of model BChEs, that it occurs within an entire parasite lineage is noteworthy and will be
311 investigated further.
312
313 The transcript levels of each *smche* varied among parasite developmental stages and this is
314 likely a response to the differing cholinergic and cholinesterase-independent requirements of
315 the parasite throughout its lifecycle. For example *smache1* is expressed at a higher level in
316 adult males than females, probably due to the more "muscular" roles of attachment and

bioRxiv preprint doi: https://doi.org/10.1101/583658; this version posted March 21, 2019. The copyright holder for this preprint (which was not certified by peer review) is the author/funder, who has granted bioRxiv a license to display the preprint in perpetuity. It is made available under aCC-BY-NC-ND 4.0 International license.

317 movement orchestrated by the male compared to the female, which remains sedentary once
318 inside the gynecophoric canal of the male [34]. Expression of *smbche1* was highest in the egg
319 stage; there is evidence for BChE involvement in chicken embryo neurogenesis and
320 development, independent of its enzymatic function [35], which suggests that *Sm*BChE1 could
321 play a role in parasite embryogenesis. The miracidium and sporocyst stages had the highest
322 levels of *smache3* expression, in agreement with Parker-Manuel et al [36].
323
324 Immunolocalization of the *Sm*ChEs revealed expression in the neuromusculature and tegument
325 to varying degrees, depending on the paralog, and is consistent with early localization
326 experiments [20], although the antibodies used in those studies were raised against AChEs
327 purified from parasite extracts and so the localization could not be attributed to a specific family
328 member. Localization to the neuromusculature relates to the proteins' traditional cholinergic
329 functions whereas tegumental distribution is suggestive of non-neuronal cholinergic and/or
330 non-cholinergic roles. Indeed, surface-expressed *Sm*AChE has been implicated in mediating
331 glucose scavenging by the parasite, as this process can be ablated by membrane-impermeable
332 AChE inhibitors [22, 23]. Tegumental *Sm*AChE may also act to hydrolyze exogenous ACh,
333 neutralizing its immune-mediating function to create an environment more conducive to
334 parasite establishment [31]. The localization of these proteins to the tegument of schistosomula
335 should also be noted since early developing schistosomula are considered most vulnerable to
336 immune attack [37], and so *Sm*AChE-targeted immunotherapeutics could be used effectively
337 to vaccinate against schistosomiasis. Indeed, antibodies against *Sm*AChEs have been shown to
338 interact with the surface of schistosomula, resulting in complement-dependent killing of the
339 parasite [38].
340

bioRxiv preprint doi: https://doi.org/10.1101/583658; this version posted March 21, 2019. The copyright holder for this preprint (which was not certified by peer review) is the author/funder, who has granted bioRxiv a license to display the preprint in perpetuity. It is made available under aCC-BY-NC-ND 4.0 International license.

341 Full-length and functional *Sm*ChEs were expressed in *P. pastoris*. *Sm*AChE1 had preferred
342 substrate specificity for AcSCh over BcSCh, albeit at a three-fold lower affinity than previously
343 reported for *Sm*AChE1 expressed in *Xenopus laevi*s oocytes [15]. *Sm*AChE3 also had a
344 substrate preference for AcSCh and an affinity twice that of *Sm*AChE1. Extremely low enzyme
345 activity was observed with *Sm*BChE1 when AcSCh was used as a substrate, but enzymatic
346 activity significantly increased with the use of BcSCh as the substrate. Although sequence
347 alignment of *Sm*BChE1 with the other two *Sm*ChEs revealed a single amino acid substitution
348 in the peripheral anionic site (Glu – Trp), acyl binding pocket (Val – Leu) and catalytic triad
349 (His – Gln), it was unclear whether these changes alone were enough to classify *Sm*BChE1 as
350 a BChE; based on the significant difference in substrate preference, however, this classification
351 would appear valid. Cloning of a recombinant BChE from *S. mansoni* is consistent with our
352 observations of BChE activity in parasite extracts, and *S. mansoni* schistosomula exhibited
353 significantly more activity than adults, as did *S. mansoni* compared to *S. haematobium* adults.
354 It has been reported that *S. mansoni* is more sensitive to the BChE inhibitor, iso-OMPA, than
355 *S. haematobium* [39] and it may be due to the increased BChE activity in *S. mansoni*. Indeed,
356 this relationship has been documented between AChE and metrifonate (precursor of DDVP
357 used in this study); *S. haematobium* is more sensitive to the inhibitor than *S. mansoni* because
358 of the greater amount of AChE on the worm's surface [39].
359
360 For the first time, we document the presence of secreted *Sm*ChE activity in schistosomes and
361 AChE activity was highest in cercarial ES products. Of the intra-mammalian stages tested,
362 AChE activity was highest in schistosomula and adults and may be acting to bind and neutralize
363 exogenous AChE inhibitors [40] (thus protecting tegumental and somatic AChE) or host-
364 derived ACh to mitigate the immunomodulatory effects of this molecule. Extending this
365 hypothesis, ES products from cultured female worms had lower AChE activity than males and

bioRxiv preprint doi: https://doi.org/10.1101/583658; this version posted March 21, 2019. The copyright holder for this preprint (which was not certified by peer review) is the author/funder, who has granted bioRxiv a license to display the preprint in perpetuity. It is made available under aCC-BY-NC-ND 4.0 International license.

366 could be due to females worms having less of a requirement for this defensive mechanism as
367 they reside in the relative shelter of the gynecophoric canal. BChE activity was present in the
368 ES products of adults, schistosomula and cercariae and was significantly higher in the intra-
369 mammalian larval stage than the other two stages. The *Sm*ChE molecules present in ES were
370 isolated by purification on edrophonium (a reversible ChE inhibitor) sepharose and, consistent
371 with the class of activity observed in ES, identified by mass spectrometry as *Sm*AChE1 and
372 *Sm*BChE1; the former being forty-fold more abundant than the latter.
373
374 RNAi-mediated silencing of *smache1* and *smache3* in schistosomula showed decreases in
375 AChE activity, consistent with reductions in transcript and protein expression levels.
376 Moreover, inhibition of this biochemical activity was greater in schistosomula treated with the
377 *smche* siRNA cocktail than parasites receiving any of the individual treatments, further
378 evidence suggestive of simultaneous silencing of all *smache* paralogs. AChE activity inhibition
379 in *smache3*-silenced parasites was more pronounced than in *smache1*-silenced parasites, which
380 was inconsistent with protein level reductions and this may be due to the increased AChE
381 activity reported for *Sm*AChE1 (Vmax = 5.57 nmol/min/mg, Km = 5.83 mM) compared to
382 *Sm*AChE3 (Vmax = 5.59 nmol/min/mg, Km = 10.87 mM). It is also possible that there may
383 not be a direct correlation between AChE activity and protein expression, given that additional,
384 non-cholinergic functions have been ascribed to ChEs [5, 22, 41]. This may also be the reason
385 why no significant decrease in BChE activity was observed in *smbche1*-silenced parasites,
386 despite significant reductions in transcript and protein expression levels.
387
388 Previous studies have documented the involvement of *Sm*ChEs in the uptake of exogenous
389 glucose by schistosomes through the ablation of the glucose uptake pathway by
390 organophosphorus [39] and large molecule [23] AChE inhibitors, so we sought to identify the

bioRxiv preprint doi: https://doi.org/10.1101/583658; this version posted March 21, 2019. The copyright holder for this preprint (which was not certified by peer review) is the author/funder, who has granted bioRxiv a license to display the preprint in perpetuity. It is made available under aCC-BY-NC-ND 4.0 International license.

391 *Sm*ChE paralog(s) responsible for this mediation through the use of RNAi targeting *smche*
392 genes. Individual gene knockdown of *smache1* and *smache3* suppressed glucose uptake in
393 schistosomula, implying that both genes were involved in regulation of this mechanism.
394 Tegumental AChE is speculated to mediate glucose uptake by limiting the interaction of ACh
395 with tegumental nicotinic ACh receptors which is thought to decrease the amount of glucose
396 uptake through surface glucose transporters. The fact that both molecules are localized to the
397 tegument and can hydrolyze ACh therefore provides evidence for their role in this pathway.
398 Silencing of *smbche1* in schistosomula did not show any difference in glucose uptake and is
399 probably reflective of the molecule's limited role in ACh hydrolysis. Transcript levels of *sgtp1*
400 and *sgtp4* were not significantly changed in *smache1*- and *smache3*-silenced parasites,
401 suggesting that *Sm*AChEs may facilitate glucose uptake in a manner which does not directly
402 involve glucose transporters. Indeed, at least in nematodes, AChEs have been proposed to be
403 involved in altering the permeability of surrounding host cells, allowing nutrients (such as
404 glucose) to leak into the parasite niche and be uptaken [42].

405

406 Individual *smche* silencing in schistosomula resulted in significant decreases in parasite
407 viability at various timepoints after treatment, with *smache3*-silenced parasites showing the
408 most rapid and significant decrease in viability after treatment. Of the *smche* paralogs studied,
409 *smche3* is the only one whose expression is significantly upregulated between *S. mansoni*
410 cercariae and schistosomula [36], an observation consistent with qPCR data, and so silencing
411 this relatively highly expressed gene may have the most profound effects of all *smche* silencing
412 on parasite viability. The viability of parasites treated with all three *smche* siRNAs was
413 significantly decreased compared to parasites treated with an individual siRNA, suggesting
414 functional overlap exists between the paralogs. This redundancy has been documented in
415 AChE-knockout mice where BChE has the ability to hydrolyze ACh in the absence of AChE

bioRxiv preprint doi: https://doi.org/10.1101/583658; this version posted March 21, 2019. The copyright holder for this preprint (which was not certified by peer review) is the author/funder, who has granted bioRxiv a license to display the preprint in perpetuity. It is made available under aCC-BY-NC-ND 4.0 International license.

[43, 44]. Moreover, AChE deletion is found to be lethal in *Drosophila* only because there is no alternative BChE paralog to compensate for the lack of ACh hydrolysis [45, 46]. Similar to the observations in this study, simultaneous knockdown of multiple ChE genes has been reported to have deleterious effects on their target organisms including the insects *Plutella xylostella* [47], *Chilo suppressalis* [48] and *Tribolium castaneum* [49] and the nematodes *Nippostrongylus brasiliensis* [50] and *Caenorhabditis elegans* [51]. Similarly, chemotherapy with "broad spectrum" ChE inhibitors has shown to be effective against a range of organisms, including pest insects [52], schistosomes [23, 53-55] and parasitic nematodes [56]. It is likely that the simultaneous silencing of the *smche* genes in this study has a profound effect on parasite viability due to the knockdown of cholinergic signaling, a process to which all paralogs contribute, as they have all been shown to hydrolyze ChE substrates. Also possible is that knockdown of these three genes might have resulted in the ablation of multiple other functions that have been suggested for these molecules [5, 49, 57]. Reflective of *in vitro* silencing experiments, worm recovery from mice infected with all groups of *smche*-silenced parasites was significantly less than controls, indicating that suppression of *smache1*, *smbche1* or *smache3* could inhibit schistosome establishment and/or development in the host. An immunomodulatory function that results in a host environment favorable to parasite survival has been suggested for AChE secreted by *N. brasiliensis* [31] and so it may be that, if schistosome ChEs have similar non-neuronal roles, impairment of ChE function in these parasites may lead to more efficient immune-mediated worm expulsion. There is now a growing body of evidence that AChEs play non-classical roles as adhesion molecules [4, 58, 59] due to these two protein families sharing significant domain homology and so *Sm*ChE-silenced worms may be unable to properly establish in their site of predilection due to impaired adherence to host vasculature. Indeed, *in vivo* treatment with AChE-inhibitory tris (p-aminophenyl) carbonium salts [60] results in a shift of the worms from the mesenteries to the

bioRxiv preprint doi: https://doi.org/10.1101/583658; this version posted March 21, 2019. The copyright holder for this preprint (which was not certified by peer review) is the author/funder, who has granted bioRxiv a license to display the preprint in perpetuity. It is made available under aCC-BY-NC-ND 4.0 International license.

liver, which may be a consequence of improper parasite attachment. Schistosomula silenced for all three *smche* genes exhibited the highest mortality *in vivo* when worm recovery was averaged across the two independent trials, suggesting that, not only is simultaneous knockdown of *Sm*ChEs required to overcome any functional redundancy between the molecules, but that this treatment has the largest impact on parasite pathogenesis due to the inhibition of multiple biological functions collectively orchestrated by these proteins.

The *smche* transcript levels of silenced worms recovered from mice were no different from control parasites and it is likely that the surviving worms received less siRNA than those worms that died in the host. Alternatively, surviving worms might have recovered from the transient effects of RNAi, highlighting the advantage of targeted gene knockout techniques such as CRISPR/Cas9 which has recently been reported for the first time in schistosomes [61].

It is generally accepted that vertebrate BChE has a predominant role in the detoxification of ingested or inhaled drugs and poisons such as the AChE-inhibitory organophosphorous esters that constitute nerve agents and pesticides due to the binding of the enzyme to these molecules (reviewed in [3]). Inactivation of *Sm*BChE1 in parasite extracts and live schistosomula by the BChE inhibitor iso-OMPA or through RNAi-mediated silencing potentiated the effects of DDVP whereas addition of exogenous *Sm*BChE1 mitigated the effects, suggesting a similar detoxification role exists for schistosome BChE as for the vertebrate enzyme. Numerous plant species in the *Solanaceae* used for their nutritional value (potatoes, for example) and others employed in traditional medicine for their anthelmintic properties contain naturally-occurring AChE-inhibitory compounds [62, 63], and so it may be that the evolution of this dietary behavior in schistosomiasis endemic populations has resulted in selective pressure on the

bioRxiv preprint doi: https://doi.org/10.1101/583658; this version posted March 21, 2019. The copyright holder for this preprint (which was not certified by peer review) is the author/funder, who has granted bioRxiv a license to display the preprint in perpetuity. It is made available under aCC-BY-NC-ND 4.0 International license.

parasite to produce these particular ChE molecules. The localization of *Sm*BChE1 to the tegument and its presence in ES products may further support this hypothesis, as the enzyme would be spatially available to interact with toxins present in the host environment, thus safeguarding parasite AChE against AChE inhibitors. Moreover, BChE activity is higher in *S. mansoni* than *S. haematobium*, which is more sensitive to the effects of the organophosphorous AChE inhibitor metrifonate. It has been reported that this sensitivity is due to the larger amount of tegumental AChE present in *S. haematobium* [39], but it may also be due to the reduced amount of BChE available to detoxify the inhibitor, as a similar relationship has been reported in studies which use human BChE to counter organophosphate toxicity [64]. Plasma-derived human BChE is currently in a phase I clinical trial as a nerve agent detoxifier, and a recombinant human BChE mutant is being used to prevent relapse in cocaine addicts due to the enzyme's ability to hydrolyze the drug into inactive by-products [3]. One of the major limitations of these approaches, however, is the catalytic turnover of human BChE [3] and so there is emphasis on the identification of BChE homologues from other organisms, such as *Sm*BChE1, that might offer improved detoxification activity in this regard.

Inhibition of BChE in the absence of DDVP results in parasite death so a bio-scavenging role is possibly not the only function of this enzyme. Indeed, vertebrate BChE has also been shown to have roles in (1) ACh hydrolysis in situations of AChE deficiency [65], (2) fat metabolism by hydrolyzing the feeding stimulant peptide octanoyl ghrelin [66], and (3) scavenging polyproline-rich peptides to regulate protein-protein and protein-DNA interactions [67].

In summary, the work herein has identified multiple ChE paralogs in the genome of *S. mansoni* where previous studies, making use of the technology available at the time, attributed ChE activity to a single AChE. Consistent with previous observations that ChEs are multi-faceted

bioRxiv preprint doi: https://doi.org/10.1101/583658; this version posted March 21, 2019. The copyright holder for this preprint (which was not certified by peer review) is the author/funder, who has granted bioRxiv a license to display the preprint in perpetuity. It is made available under aCC-BY-NC-ND 4.0 International license.

enzymes, we posit that the three ChE paralogs described herein may fulfil distinct neuronal and non-neuronal functions based on their anatomical and temporal expression in the parasite and its ES products and the enzymatic activity of recombinant molecules. In addition to providing valuable insight into the functionality of individual ChE molecules, the study herein documents the essentiality of these proteins, providing a compelling evidence base for their use as intervention targets against schistosomiasis.

Materials and Methods

Ethics statement

All experimental procedures reported in the study were approved by the James Cook University (JCU) animal ethics committee (ethics approval numbers A2271 and A2391). Mice were maintained in cages in the university's quarantine facility (Q2152) for the duration of the experiments. The study protocols were in accordance with the 2007 Australian Code of Practice for the Care and Use of Animals for Scientific Purposes and the 2001 Queensland Animal Care and Protection Act.

Parasite maintenance, culture and ES collection

Biomphalaria glabrata snails infected with *S. mansoni* (NMRI strain) were obtained from the Biomedical Research Institute (BRI), MD, USA. Cercariae were shed from infected snails through exposure to light at 28°C for 1.5 h and were mechanically transformed into schistosomula [68]. To obtain adult worms, 6-8 week old male BALB/c mice (Animal Resource Centre, WA, Australia) were infected with 180 cercariae via tail penetration and adults were harvested by vascular perfusion at 7-8 weeks post-infection [69]. Both adult worms and schistosomula were cultured (10 adult pairs/ml and 2000 schistosomula/ml) at 37°C and 5% CO_2 in serum-free modified Basch medium [70] supplemented with 4 × antibiotic/antimycotic

bioRxiv preprint doi: https://doi.org/10.1101/583658; this version posted March 21, 2019. The copyright holder for this preprint (which was not certified by peer review) is the author/funder, who has granted bioRxiv a license to display the preprint in perpetuity. It is made available under aCC-BY-NC-ND 4.0 International license.

(AA - 200 units/ml penicillin, 200 µg/ml streptomycin and 0.5 µg/ml amphotericin B) (SFB) in 6 well plates. Media containing ES products was initially collected after 3 h for schistosomula or 24 h for adults, and replenished daily thereafter. ES products were stored at -80°C. Media was thawed when needed, concentrated through Amicon centrifugation filters (Sigma) with a 3 kDa molecular weight cutoff (MWCO), buffer exchanged into phosphate buffered saline, pH 7.4 (PBS) and aliquoted. Protein concentration of ES products was determined using the Pierce BCA™ Protein Assay kit (Thermofisher). To collect cercarial ES products, freshly-shed cercariae were incubated in H_2O (4000/ml) at 25°C for 3 h. H_2O was filtered through Whatman filter paper (11 µm) to remove cercariae and associated debris, and ES products were concentrated, quantified and stored as described for adult and schistosomula ES products.

Parasite extract preparation

To make PBS-soluble extracts, worms were homogenized in PBS (50 µl/adult worm pair or 50 µl/1000 schistosomula) at 4°C using a TissueLyser II (Qiagen), homogenates were incubated overnight with mixing at 4°C and the supernatants collected by centrifugation at 15,000 *g* for 1 h at 4°C. Triton X-100-soluble extracts were made from the PBS-insoluble pellets by resuspension in 1% Triton X-100, 40 mM Tris-HCl, pH 7.4, mixing overnight at 4°C and the supernatant collected by centrifugation at 15,000 *g* for 1 h at 4°C. Tegument extraction was achieved using a combination of freeze/thaw/vortex [71]. In brief, parasites were slowly thawed on ice, washed in TBS (10 mM Tris/HCl, 0.84% NaCl, pH 7.4) and incubated for 5 min on ice in 10 mM Tris/HCl, pH 7.4 followed by vortexing (5 × 1 s bursts). Subsequently, the tegumental extract was pelleted at 1000 *g* for 30 min and solubilized (3×) in 200 µl of 0.1% (w/v) SDS, 1% (v/v) Triton X-100 in 40 mM Tris, pH 7.4 with pelleting at 15,000 *g* between each wash. Protein concentration was determined using the Pierce BCA Protein Assay kit, aliquoted and stored at -80°C until use.

bioRxiv preprint doi: https://doi.org/10.1101/583658; this version posted March 21, 2019. The copyright holder for this preprint (which was not certified by peer review) is the author/funder, who has granted bioRxiv a license to display the preprint in perpetuity. It is made available under aCC-BY-NC-ND 4.0 International license.

Bioinformatics

Based on Pfam analysis (search = cholinesterase) of the *S. mansoni* genome (http://www.geneDB.org/Homepage/Smansoni), three *smche* paralogs (*smache1* - Smp_154600, *smbche1* - Smp_125350 and *smache3* - Smp_136690) were identified. Homologous ChE sequences from other species were identified using BLASTP. (http://blast.ncbi.nlm.nih.gov/Blast.cgi) and the resulting sequences were used to generate a multiple sequence alignment using Clustal Omega (https://www.ebi.ac.uk/Tools/msa/clustalo/). MEGA 7 was used to generate a neighbor-joining tree with the Poisson correction distance method and a bootstrap test of 1,000 replicates [72]. The tree was visualized with The Interactive Tree of Life (iTOF) online phylogeny tool (https://itol.embl.de/). Structure-homology 3D models of *Sm*ChEs were generated using the I-TASSER server (http://zhanglab.ccmb.med.umich.edu/I-TASSER/). For structure visualization and catalytic triad analyses, the Accelrys Discovery Studio (Accelerys Inc.) and UCSF Chimera MatchMaker ver. 1.4 (University of California) software packages were utilized.

Real-time qPCR

Real-time qPCR was used to assess developmental expression of *smche* genes and to determine *smche* transcript suppression resulting from RNAi experiments. RNA from miracidia, sporocysts, cercariae, adult male worms, adult female worms, and eggs were obtained from BRI. Schistosomula were cultured as described above, harvested (1,000 parasites) after either 3 h, 24 h, 3 or 5 days, washed three times in PBS and stored at -80°C until use. Schistosomula from RNAi experiments were similarly processed. Total RNA extraction was performed using the Trizol (Thermofisher) reagent according to manufacturer's instructions. After air-drying, RNA pellets were re-suspended in 12 µl diethylpyrocarbonate (DEPC)-treated

bioRxiv preprint doi: https://doi.org/10.1101/583658; this version posted March 21, 2019. The copyright holder for this preprint (which was not certified by peer review) is the author/funder, who has granted bioRxiv a license to display the preprint in perpetuity. It is made available under aCC-BY-NC-ND 4.0 International license.

565 water. Concentration and purity of RNA was determined using an ND2000 Nanodrop
566 spectrophotometer (Thermofisher). Synthesis of cDNA was carried out with 1 µg of total RNA
567 using Superscript-III-Reverse Transcriptase (Invitrogen) according to the manufacturer's
568 instructions. Finally, cDNA was quantified, diluted to 50 ng/µl, aliquoted and stored at -20°C.
569 Real-time qPCR primers for each *smche* (supplementary Table 1) were designed using
570 Primer3 (http://frodo.wi.mit.edu/). The housekeeping gene *smcox1* was selected as an internal
571 control to normalize relative *smche* gene expression [73]. Each qPCR (1 µl (50 ng) of cDNA,
572 5 µl of 2x SYBR green master mix (Bioline), 1µl (5 pmol/µl) each of forward and reverse
573 primers and 2 µl of nuclease-free water) was run in a Rotor-Gene Q thermal cycler (Qiagen)
574 using 40 cycles of 95°C for 10 seconds, 50-55°C for 15 seconds and 72°C for 20 seconds.
575 Stage-specific *smche* gene expression levels were normalized against *smcox1*gene expression
576 using the comparative $2^{-\Delta\Delta CT}$ method [74]. All results represent the average of 5 independent
577 experiments with data presented as mean ± SEM.
578
579 ***Cloning, expression and purification of smche gene fragments in E. coli***
580 Complete ORFs for *smache1*, *smbche1* and *smache3* were synthesized by Genewiz. Attempts
581 to express full-length sequences in *E. coli* were unsuccessful, so primer sets incorporating *Nde*I
582 (forward primer) and *Xho*I restriction enzyme sites (reverse primer) were designed
583 (supplementary Table 1) to amplify partial, non-conserved regions of each *smche*, which might
584 prove more amenable to expression. Sequences (containing *Nde*I/ *Xho*I sites) for each p*Sm*ChE
585 were amplified from each full-length template by PCR and cloned into the pET41a expression
586 vector (Novagen) such that the N-terminal GST tag was removed. Protein expression was
587 induced for 24 h in *E. coli* BL21(DE3) by addition of 1 mM Isopropyl beta-D-1-
588 thiogalactopyranoside (IPTG) using standard methods. Cultures were harvested by
589 centrifugation (8,000 *g* for 20 min at 4°C), re-suspended in 50 ml lysis buffer (50 mM sodium

bioRxiv preprint doi: https://doi.org/10.1101/583658; this version posted March 21, 2019. The copyright holder for this preprint (which was not certified by peer review) is the author/funder, who has granted bioRxiv a license to display the preprint in perpetuity. It is made available under aCC-BY-NC-ND 4.0 International license.

590 phosphate, pH 8.0, 300 mM NaCl, 40 mM imidazole) and stored at -80°C. Cell pellets were
591 lysed by three freeze-thaw cycles at -80°C and 42°C followed by sonication on ice (10 × 5 s
592 pulses [70% amplitude] with 30 s rest periods between each pulse) with a Qsonica Sonicator.
593 Triton X-100 was added to each lysate at a final concentration of 3% and incubated for 1 h at
594 4°C with end-over-end mixing. Insoluble material (containing r*Sm*ChEs) was pelleted by
595 centrifugation at 20,000 *g* for 20 min at 4°C. The supernatant was discarded, and inclusion
596 bodies (IBs) were washed twice by resuspension in 30 ml of lysis buffer followed by
597 centrifugation at 20,000 *g* for 20 min at 4°C. IBs were then solubilized sequentially by
598 resuspension in 25 ml lysis buffers containing either 2 M, 4 M or 8 M urea, end-over-end
599 mixing overnight at 4°C and centrifugation at 20,000 *g* for 20 min at 4°C. Finally, supernatant
600 containing solubilized IBs was diluted 1:4 in lysis buffer containing 8M urea and filtered
601 through a 0.22 µm membrane (Millipore). Solubilized IBs were purified by immobilized metal
602 affinity chromatography (IMAC) by loading onto a prepacked 1 ml His-Trap HP column (GE
603 Healthcare) equilibrated with lysis buffer containing 8M urea at a flow rate of 1 ml/min using
604 an AKTA-pure-25 FPLC (GE Healthcare). After washing with 20 ml lysis buffer containing
605 8M urea, bound His-tagged proteins were eluted using the same buffer with a stepwise gradient
606 of 50-250 mM imidazole (50 mM steps). Fractions containing r*Sm*ChEs (as determined by
607 SDS-PAGE) were pooled and concentrated using Amicon Ultra-15 centrifugal devices with a
608 3 kDa MWCO and quantified using the Pierce BCA Protein Assay kit. The final concentration
609 of each r*Sm*ChE was adjusted to 1 mg/ml and proteins were aliquoted and stored at -80°C.
610
611 ***Generation of anti-rSmChE antisera and purification of IgG***
612 Three groups of five male BALB/c mice (6-week-old) were intraperitoneally immunized with
613 either r*Sm*AChE1, r*Sm*BChE1 or r*Sm*AChE3 subunits (50 µg/mouse). Antigens were mixed
614 with an equal volume of Imject alum adjuvant (Thermofisher) and administered three times,

bioRxiv preprint doi: https://doi.org/10.1101/583658; this version posted March 21, 2019. The copyright holder for this preprint (which was not certified by peer review) is the author/funder, who has granted bioRxiv a license to display the preprint in perpetuity. It is made available under aCC-BY-NC-ND 4.0 International license.

615 two weeks apart. Two weeks after the final immunization, mice were sacrificed and blood was
616 collected via cardiac puncture. Blood from all mice in each group was pooled and serum was
617 separated by centrifugation after clotting and stored at −20°C. Polyclonal antibodies were
618 purified from mouse sera using Protein A Sepharose-4B (Thermofisher) according to the
619 manufacturer's instructions. Serum from naïve mice was similarly processed.

620

621 ***Immunolocalization using anti-rSmChE antisera***

622 ***Adult worm sections***: Freshly perfused adult *S. mansoni* and *S. haematobium* worms were fixed
623 in 4% paraformaldehyde, embedded in paraffin and sections (7 μm thick) were cut in a cryostat.
624 Following deparaffinization in xylene and rehydration in an ethanol series, antigen retrieval
625 was performed by boiling the slides in 10 mM sodium citrate, pH 6.0, for 40 min followed by
626 a solution of 10 mM Tris, 1 mM EDTA, 0.05% Tween, pH 9.0, for 20 min. All sections were
627 then blocked with 10% heat-inactivated goat serum for 1 h RT. After washing 3 times with
628 PBST, sections were incubated with anti-*Sm*AChE1, anti-*Sm*BChE1, anti-*Sm*AChE3, naïve
629 sera (negative control), *S. mansoni* or *S. haematobium* infected mouse sera (positive controls)
630 (1:50 in PBST) overnight at 4°C and then washed again (3 × 5 min each).
631 Finally, the sections were incubated with goat-anti-mouse IgG-alexafluor647 (Sigma) (1:200
632 in PBST) for 1 h in the dark at RT. After a final washing step, slides were mounted with
633 coverslips in Entellan mounting medium (Millipore). Fluorescence and bright-field microscopy
634 were performed with an AxioImager M1 fluorescence microscope (Zeiss) using 10× and 20×
635 objectives.

636 ***Live schistosomula:*** *In vitro* cultured living cercariae and schistosomula (3 h, 24 h, 3 and 5
637 days old) were harvested, washed with PBS and then blocked with PBST/10% heat-inactivated
638 goat serum for 30 min at RT. Following three washes, the larvae were incubated with anti-
639 *Sm*AChE1, anti-*Sm*BChE1, anti-*Sm*AChE3 or naïve serum (negative control) (1:100 in PBST)

bioRxiv preprint doi: https://doi.org/10.1101/583658; this version posted March 21, 2019. The copyright holder for this preprint (which was not certified by peer review) is the author/funder, who has granted bioRxiv a license to display the preprint in perpetuity. It is made available under aCC-BY-NC-ND 4.0 International license.

640 overnight at 4°C. Parasites were washed again before incubation with goat-anti-mouse IgG-
641 alexafluor647 (Sigma) (1: 200 in PBST) for 1 h in the dark at RT, followed by 3 washes.
642 Finally, schistosomes were fixed in 4% paraformaldehyde and transferred to a microscope slide
643 for fluorescence microscopy using an AxioImager M1 fluorescence microscope.
644
645 ***Cloning and expression of full-length SmChEs in P. pastoris***
646 Full-length sequences (minus the signal peptide) of *Sm*AChE1, *Sm*BChE1 and *Sm*AChE3
647 (f*Sm*ChEs) were *Eco*RI/*Xba*I cloned into the C-terminal 6-His-tagged pPICZαA expression
648 vector (Invitrogen) to facilitate secretory expression. Recombinant plasmids (20 µg) were
649 linearized with *Pme*l (f*Sm*AChE1 & f*Sm*BChE1) and *Sac*I (f*Sm*AChE3), purified by ethanol
650 precipitation and resuspended in 15 µl of H_2O. Linearized vectors were electroporated
651 according to the manufacturer's instructions into *P. pastoris* X-33 cells (Thermofisher) in 2
652 mm cuvettes (2 ms, 2000V, 25 µF, 200 Ω, square wave pulse), using a Gene Pulser Xcell (Bio-
653 Rad), plated onto YPDS agar plates containing 100 µg/ml zeocin and incubated for 3 days at
654 30°C. Resultant colonies were then picked and patched onto YPDS agar containing 2 mg/ml
655 zeocin and plates incubated at 30°C until colonies were visible. A high-expressing clone of
656 each r*Sm*ChE (determined from pilot expression experiments) was used to inoculate 5 ml
657 BMGY media supplemented with 50 ug/ml zeocin and grown overnight at 30°C with rotation
658 at 250 rpm. The entire culture was then used to inoculate 250 ml of BMGY in a 2L baffled
659 flask and incubation was continued for 24 h at 30°C. Cells were pelleted at 5000 *g* for 20 min
660 at RT, re-suspended in 1L of BMMY (to induce protein expression) and split between 2 ×
661 2L baffled flasks, which were incubated with shaking (250 rpm) at 30°C for 72 h. Methanol
662 was added to a final concentration of 0.5% (2.5 ml/flask) every 24 h to maintain induction of
663 protein expression. Culture medium containing the secreted f*Sm*ChE proteins was harvested
664 by centrifugation (5000 *g* for 20 min at RT) and filtered through a 0.22 µm membrane filter

bioRxiv preprint doi: https://doi.org/10.1101/583658; this version posted March 21, 2019. The copyright holder for this preprint (which was not certified by peer review) is the author/funder, who has granted bioRxiv a license to display the preprint in perpetuity. It is made available under aCC-BY-NC-ND 4.0 International license.

(Millipore). Recombinant proteins were purified by IMAC using an AKTA-pure-25 FPLC (GE Healthcare). Briefly, culture medium was loaded onto a 5 ml His-excel column, pre-equilibrated with binding buffer (50 mM PBS pH 7.4, 300 mM NaCl), washed with 20 column volumes of binding buffer and then eluted with binding buffer containing a linear imidazole gradient (20 to 500 mM). The purity of fractions within the main peak was analyzed by SDS-PAGE and fractions of appropriate purity were pooled, concentrated and buffer exchanged into PBS using Amicon Ultra-15 centrifugal devices with a 3 kDa MWCO and quantified using the Pierce BCA Protein Assay kit. The final concentration of each f*Sm*ChE was adjusted to 1 mg/ml and proteins were aliquoted and stored at -80°C.

SmChE enzyme assays

Activity of f*Sm*ChEs, extracts and ES samples was determined by the Ellman method [75]; modified for use with 96 well microplates. Samples (parasite extracts, ES and f*Sm*ChEs) were diluted in assay buffer (0.1M sodium phosphate, pH 7.4), and 2 mM acetylthiocholine (AcSCh) or butyrylthiocholine (BcSCh) (Sigma) and 0.5 mM 5, 5'-dithio-bis (2-nitrobenzoic acid) (DTNB) (Sigma) was added. The absorbance increase was monitored every 5 min at 405 nm in a Polarstar Omega microplate reader (BMG Labtech). Specific activity was calculated using the initial velocity of the reaction and extinction coefficient of 13,260 M^{-1} cm^{-1} for TNB. To investigate sensitivity of parasite ES products to AChE inhibitors, 25 µg of adult ES was pre-treated with 1 µM DDVP - active metabolite of the organophosphorous AChE inhibitor metrifonate - for 20 min at RT before measuring activity. Kinetic parameters of f*Sm*ChEs were characterized by measuring enzyme activity at differing substrate concentrations and plotting enzyme activity [V] vs. substrate concentration [S]. The Km ([S] at 1/2 Vmax) was calculated using the Michaelis Menton equation. Enzyme assays with inhibitors were performed as above except that f*Sm*ChEs in assay buffer were pre-treated with 1 µM DDVP, in the case of

bioRxiv preprint doi: https://doi.org/10.1101/583658; this version posted March 21, 2019. The copyright holder for this preprint (which was not certified by peer review) is the author/funder, who has granted bioRxiv a license to display the preprint in perpetuity. It is made available under aCC-BY-NC-ND 4.0 International license.

f*Sm*AChE1 and f*Sm*AChE3, or 1 mM iso-OMPA – a membrane-impermeable specific BChE inhibitor - in the case of f*Sm*BChE1, for another 20 min at RT. Experiments were performed in triplicate with data presented as the mean ± SEM.

Purification of secreted SmChEs from adult S. mansoni ES products

Affinity chromatography using edrophonium chloride-sepharose was used to purify *Sm*AChE from *S. mansoni* based on the method of Hodgson and Chubb [76]. Briefly, 1 g of epoxy-activated sepharose 6B beads was washed with distilled H_2O, the slurry centrifuged at 814 *g* for 5 min and the pellet gently resuspended in 50 mM sodium phosphate, pH 8.0, containing 200 mM edrophonium chloride (1:2 ratio of sepharose:edrophonium chloride). The pH of the solution was adjusted to 10.0 and coupling of edrophonium with the sepharose was facilitated by incubating the mixture overnight with shaking at 50°C. The gel was then washed sequentially with 10 volumes each of 100 mM sodium acetate, pH 4.5, 12 mM sodium borate, pH 10.0, and distilled H_2O and finally resuspended in distilled H_2O to generate a 1 ml gel slurry. The gel slurry was packed into a chromatography column (10 cm long, 1 cm diameter) and equilibrated by gravity flow at 4°C with 10 column volumes (CV) of equilibration buffer (50 mM phosphate buffer, pH 8.0). Approximately 20 ml of ES from adult *S. mansoni* (concentrated through a 10 kDa MWCO centrifugal filter from a starting volume of 500 ml of media, harvested each day for 7 days from 100 pairs of adult worms and buffer exchanged into equilibration buffer) was added to the column followed by washes with 20 CV of equilibration buffer and 20 CV of equilibration buffer containing 500 mM NaCl. Bound *Sm*ChE was then eluted with 10 CV of equilibration buffer containing 500 mM NaCl and 20 mM edrophonium chloride. The eluate was concentrated and buffer exchanged into PBS using a 10 kDa MWCO centrifugal filter (edrophonium chloride is an AChE inhibitor and would interfere with

bioRxiv preprint doi: https://doi.org/10.1101/583658; this version posted March 21, 2019. The copyright holder for this preprint (which was not certified by peer review) is the author/funder, who has granted bioRxiv a license to display the preprint in perpetuity. It is made available under aCC-BY-NC-ND 4.0 International license.

714 subsequent activity assays) and resolved by 10% SDS-PAGE to check purity and facilitate
715 identification by mass spectrometry.
716
717 ***Mass spectrometric analysis of purified, secreted SmChE***
718 Bands of interest were manually excised from the SDS polyacrylamide gel, washed with 50%
719 acetonitrile and dried under vacuum at 30°C. Cysteine residues were reduced with 20 mM
720 DTT for 1 h at 65°C followed by alkylation with 50 mM iodoacetamide for 40 min at 37°C in
721 the dark. In-gel trypsin digestion was performed at 37°C overnight with 0.8 ng of trypsin in
722 trypsin reaction buffer (40 mM ammonium bicarbonate, 9% acetonitrile). The supernatant
723 was removed to a fresh microfuge tube and stored at 4°C, and the remaining peptides were
724 further extracted from the gel pieces by incubation with 0.1% trifluoracetic acid (TFA) at
725 37°C for 45 min. The newly extracted supernatant was combined with the previously collected
726 supernatant, then dried under vacuum. Prior to the matrix-assisted laser desorption/ionization-
727 time-of-flight mass spectrometry (MALDI-TOF MS) analysis, peptides were concentrated and
728 desalted using ZipTips (Millipore) following the manufacturer's instructions. Tryptic peptides
729 were re-dissolved in 10 µl 5% formic acid and 6 µl was injected onto a 50 mm 300 µm C18
730 trap column (Agilent Technologies) followed by an initial wash step with Buffer A (5% (v/v)
731 ACN, 0.1% (v/v) formic acid) for 5 min at 30 µl/min. Peptides were eluted at a flow rate of 0.3
732 µl/min onto an analytical nano HPLC column (15 cm × 75 µm 300SBC18, 3.5 µm, Agilent
733 Technologies). The eluted peptides were then separated by a 55-min gradient of buffer B (90/10
734 acetonitrile/ 0.1% formic acid) 1-40% followed by a 5 min steeper gradient from 40-80%. The
735 mass spectrometer (ABSciex 5600 Triple Tof) was operated in data-dependent acquisition
736 mode, in which full scan TOF-MS data was acquired over the range of 350-1400 m/z, and over
737 the range of 80-1400 m/z for product-ion observed in the TOF-MS scan exceeding a threshold

bioRxiv preprint doi: https://doi.org/10.1101/583658; this version posted March 21, 2019. The copyright holder for this preprint (which was not certified by peer review) is the author/funder, who has granted bioRxiv a license to display the preprint in perpetuity. It is made available under aCC-BY-NC-ND 4.0 International license.

738 of 100 counts and a charge state of +2 to +5. Analyst 1.6.1 (ABSCIEX) software was used for
739 data acquisition and analysis.
740 For protein identification, a database was built using the *S. mansoni* genome
741 v5.0 [http://www.genedb.org/Homepage/Smansoni] with the common repository of
742 adventitious proteins (cRAP, http://www.thegpm.org/crap/) appended to it. Mascot v.2.5.1
743 (Matrix Science) was used for database search. Carbamidomethylation of Cys was set as a fixed
744 modification and oxidation of Met and deamidation of Asn and Gln were set as variable
745 modifications. MS and MS/MS tolerance were set at 10 ppm and 0.1 Da, respectively and
746 only proteins with at least two unique peptides (each composed of at least seven amino acid
747 residues) identified were considered reliably identified and used for analysis.
748
749 ***siRNA design and synthesis***
750 Three short interfering RNA duplexes (siRNAs) targeting each of the three identified *smche*
751 paralogs were designed (supplementary Table 2) and checked to avoid off-target silencing
752 by BLAST search using the *S. mansoni* genome. An irrelevant siRNA from firefly luciferase
753 (*luc*) was selected as a negative control [77]. All siRNAs were commercially synthesized
754 (Integrated DNA Technologies) and oligonucleoitdes were suspended to a concentration of 1
755 µg/µl in DEPC-treated water.
756
757 ***Electroporation of schistosomula with siRNA***
758 Prior to electroporation, mechanically transformed schistosomula were cultured for 24 h (2,000
759 schistosomula/ml), at 37°C and 5% CO_2 in SFB in 6 well plates. After 3 washes with PBS,
760 schistosomula were re-suspended in modified Basch medium (3,000 schistosomula/100 µl) and
761 3,000 schistosomula were transferred into a Genepulser 4 mm electroporation cuvette (Bio-
762 Rad) for every siRNA treatment (four) and timepoint (four for each siRNA treatment – 1, 3, 5

bioRxiv preprint doi: https://doi.org/10.1101/583658; this version posted March 21, 2019. The copyright holder for this preprint (which was not certified by peer review) is the author/funder, who has granted bioRxiv a license to display the preprint in perpetuity. It is made available under aCC-BY-NC-ND 4.0 International license.

763 and 7 days). Schistosomula were electroporated with 10 µg of either *luc*, *smache1*, *smbche1* or
764 *smache3* siRNA or a combination of all three *smche* siRNAs (30 µg total) using a Bio-Rad
765 Gene Pulser Xcell (single 20 ms pulse – 125 V, 25 µF capacitance, 200 Ω resistance, square
766 wave electroporation) at RT, added to 24 well plates containing 1 ml pre-warmed SFB and
767 incubated (37°C, 5% CO_2) for 7 days. Schistosomula were harvested at each timepoint and
768 approximately 1,000 parasites were used for qPCR analysis (to assess transcript knockdown),
769 1,700 parasites were used for protein extract preparation (to examine phenotypic knockdown)
770 and 300 parasites were used for Trypan Blue exclusion assays (to determine parasite viability).
771 All parasite material was generated and separately analyzed from 2 independent experiments.

772

773 ***Determination of viability in siRNA-treated schistosomula***

774 Schistosomula (100 parasites/replicate) were harvested at each timepoint and viability was
775 determined by Trypan Blue exclusion staining [78]. Briefly, schistosomula were stained with
776 0.16% Trypan Blue in PBS with gentle shaking for 30 min at RT and then excess stain was
777 removed by multiple washes in PBS before fixing in 10% formalin. Parasites were counted
778 under 10× objective and live parasites (which had not taken up stain) were expressed as a
779 percentage of total worms. Each assay was performed in triplicate.

780

781 ***Evaluation of protein expression in siRNA-treated schistosomula***

782 Western blots were performed with day-7 parasite extracts (20 µg) following standard
783 procedures. The blots were probed with the anti-*Sm*ChE antibodies (1:1000 in PBST) generated
784 herein. A polyclonal anti-*Sm*-paramyosin antibody [77] was used as a loading control.

785

786

bioRxiv preprint doi: https://doi.org/10.1101/583658; this version posted March 21, 2019. The copyright holder for this preprint (which was not certified by peer review) is the author/funder, who has granted bioRxiv a license to display the preprint in perpetuity. It is made available under aCC-BY-NC-ND 4.0 International license.

787 ***Glucose uptake in schistosomula treated with siRNA***

788 In a separate RNAi experiment, newly transformed schistosomula (5,000/treatment) were
789 incubated for 5 days in SFB. Parasites were then electroporated with siRNAs as described
790 above and finally transferred to serum-free DMEM (1 mg/ml glucose) supplemented with
791 4×AA. Media (50 µl) from each experiment was collected 72 h post-treatment and the amount
792 of glucose was quantified using a colorimetric glucose assay kit (Sigma) following the
793 manufacturer's instructions. Parasite viability at this timepoint was determined by Trypan Blue
794 exclusion and transcript levels of each *smche*, as well as the glucose transporters *sgtp1* and
795 *sgtp4*, were also measured. Glucose levels were normalized according to the number of
796 parasites and expressed relative to the *luc* group. Data is the average of 2 biological and 3
797 technical replicates ± SEM.

798

799 ***Infection of mice with SmChE siRNA-treated schistosomula***

800 One-day-old schistosomula (10,000) were electroporated as above in 500 µl of SFB with 50
801 µg of either *luc*, *smache1*, *smbche1* or *smache3* siRNA or a combination of all three *smche*
802 siRNAs (150 µg total). Parasites were injected intramuscularly into both thighs (1,000 per
803 thigh) of male 6-8 week BALB/c mouse (5 mice per treatment group) using a 23-gauge needle.
804 A control group of mice were similarly injected with non-electroporated schistosomula. Adult
805 worms were perfused 20 days later to assess the number of worms that had matured and reached
806 the mesenteries. Experiments were performed independently in duplicate. After each
807 experiment, transcript levels of each *smche* from surviving worms were assessed using real-
808 time qPCR.

809

810

bioRxiv preprint doi: https://doi.org/10.1101/583658; this version posted March 21, 2019. The copyright holder for this preprint (which was not certified by peer review) is the author/funder, who has granted bioRxiv a license to display the preprint in perpetuity. It is made available under aCC-BY-NC-ND 4.0 International license.

Bio-scavenging of carboxylic esters by SmBChE1

To test the hypothesis that *Sm*BChE1 may play a role in the bio-scavenging of AChE-inhibitory molecules, we first sought to determine whether inhibition of BChE activity would potentiate the AChE-inhibitory and anti-schistosome effects of organophosphates (OP)s. Schistosomula extracts (20 µg) were diluted in assay buffer, then iso-OMPA was added to a final concentration of either 1 or 2 mM and incubated for 20 min at RT. DDVP was then added to a final concentration of 1 µM and the samples were further incubated for 20 min at RT; the final reaction volume was 180 µl. ACh (final concentration 2 mM) and DTNB (final concentration 0.5 mM) were then added and the absorbance was monitored every 5 min at 405 nm in a Polarstar Omega microplate reader (BMG Labtech). Extracts that were not treated with iso-OMPA with or without DDVP treatment were used as controls. Experiments were performed in triplicate with data presented as the mean ± SEM.

The same experiments were performed on live schistosomula using either an inhibitor- or RNAi-based approach. For the inhibitor-based experiment, 24 h schistosomula (1,000/treatment in 1 ml SFB) were pretreated with iso-OMPA at the non-lethal concentration of 100 µM and, 1 h after iso-OMPA treatment, schistosomula were treated with 1 µM DDVP and cultured for 5 h at 37°C in 5% CO_2. Parasites that were not treated with iso-OMPA but treated with DDVP were used as controls. For the RNAi-based experiment, 24 h schistosomula (1,500/100 µl SFB) were electroporated with 10 µg of either *smbche1* or *luc* siRNA as described above, added to 24 well plates containing 1 ml pre-warmed SFB and incubated (37°C, 5% CO_2) for 3 days before being treated with 1 µM DDVP and cultured for a further 5 h. For both inhibitor- and RNAi-based experiments, schistosomula viability was determined using Trypan Blue staining and data is presented as the mean ± SEM of 2 biological and 3 technical replicates.

bioRxiv preprint doi: https://doi.org/10.1101/583658; this version posted March 21, 2019. The copyright holder for this preprint (which was not certified by peer review) is the author/funder, who has granted bioRxiv a license to display the preprint in perpetuity. It is made available under aCC-BY-NC-ND 4.0 International license.

In a reverse testing of the bio-scavenging hypothesis, we sought to determine whether addition of *Sm*BChE could mitigate the effects of DDVP. Ten micrograms of f*Sm*BChE1 was pre-incubated with 1 µM final concetration DDVP in AChE assay buffer (170 µl final volume) for 20 min at RT. Schistosomula extracts (20 µg), ACh (final concentration 2 mM) and DTNB (final concentration 0.5 mM) were then added and the absorbance was monitored every 5 min at 405 nm iichlorvosn a Polarstar Omega microplate reader. Reactions without f*Sm*BChE or without DDVP were used as controls. Experiments were performed in triplicate with data presented as the mean ± SEM. Again, the same experiments were performed on live schistosomula. After the pre-treatment of different amounts of f*Sm*BChE (10, 5, and 2.5 µg) with 1 µM DDVP in 500 µl SFB, 24 h schistosomula (1,000/treatment in 500 µl SFB) were added, incubated at 37°C and 5% CO_2 for 24 h and then parasite viability was measured by Trypan Blue staining. Experiments where a similarly expressed and purified, but irrelevant, protein (*Sm*TSP2) was used instead of f*Sm*BChE, and schistosomula cultured in media alone, were used as controls. Data is presented as the mean ± SEM of 2 biological and 3 technical replicates.

Statistical analyses

Data were reported as the means ± SEM. Statistical differences were assessed using the student's *t* test. *P* values less than 0.05 were considered statistically significant.

References

1. Girard E, Bernard V, Minic J, Chatonnet A, Krejci E, Molgó J. Butyrylcholinesterase and the control of synaptic responses in acetylcholinesterase knockout mice. Life Sciences. 2007;80(24):2380-5. doi: https://doi.org/10.1016/j.lfs.2007.03.011.

2. Massoulie J, Pezzementi L, Bon S, Krejci E, Vallette FM. Molecular and cellular biology of cholinesterases. Progress in neurobiology. 1993;41(1):31-91. Epub 1993/07/01. PubMed PMID: 8321908.

bioRxiv preprint doi: https://doi.org/10.1101/583658; this version posted March 21, 2019. The copyright holder for this preprint (which was not certified by peer review) is the author/funder, who has granted bioRxiv a license to display the preprint in perpetuity. It is made available under aCC-BY-NC-ND 4.0 International license.

862 3. Lockridge O. Review of human butyrylcholinesterase structure, function, genetic
863 variants, history of use in the clinic, and potential therapeutic uses. Pharmacol Ther.
864 2015;148:34-46. Epub 2014/12/03. doi: 10.1016/j.pharmthera.2014.11.011. PubMed PMID:
865 25448037.

866 4. Silman I, Sussman JL. Acetylcholinesterase: 'classical' and 'non-classical' functions and
867 pharmacology. Curr Opin Pharmacol. 2005;5(3):293-302. Epub 2005/05/24. doi:
868 10.1016/j.coph.2005.01.014. PubMed PMID: 15907917.

869 5. Soreq H, Seidman S. Acetylcholinesterase--new roles for an old actor. Nature reviews:
870 Neuroscience. 2001;2(4):294-302. Epub 2001/04/03. doi: 10.1038/35067589. PubMed PMID:
871 11283752.

872 6. Kimber MJ, Fleming CC. Neuromuscular function in plant parasitic nematodes: a target
873 for novel control strategies? Parasitology. 2005;131(S1):S129-S42. doi:
874 10.1017/S0031182005009157.

875 7. McVeigh P, Kimber MJ, Novozhilova E, Day TA. Neuropeptide signalling systems in
876 flatworms. Parasitology. 2005;131(S1):S41-S55. doi: 10.1017/S0031182005008851.

877 8. Ribeiro P, El-Shehabi F, Patocka N. Classical transmitters and their receptors in
878 flatworms. Parasitology. 2005;131 Suppl:S19-40. Epub 2006/03/30. doi:
879 10.1017/s0031182005008565. PubMed PMID: 16569290.

880 9. Sangster NC, Song J, Demeler J. Resistance as a tool for discovering and understanding
881 targets in parasite neuromusculature. Parasitology. 2005;131(S1):S179-S90. doi:
882 10.1017/S0031182005008656.

883 10. Vermeire JJ, Humphries JE, Yoshino TP. Signal transduction in larval trematodes:
884 putative systems associated with regulating larval motility and behaviour. Parasitology.
885 2005;131(S1):S57-S70. doi: 10.1017/S0031182005008358.

886 11. Halton DW, Gustafsson MKS. Functional morphology of the platyhelminth nervous
887 system. Parasitology. 1996;113(SupplementS1):S47-S72. doi:
888 doi:10.1017/S0031182000077891.

889 12. Ribeiro P, Geary T. Neuronal signaling in schistosomes: Current status and prospects
890 for post-genomics. . Canadian Journal of Zoology/Revue Canadienne de Zoologie. 2010;88 1-
891 22.

892 13. Arnon R, Silman I, Tarrab-Hazdai R. Acetylcholinesterase of *Schistosoma mansoni* -
893 Functional correlates - Contributed in honor of Professor Hans Neurath's 90th birthday. Protein
894 Science. 1999;8(12):2553-61. PubMed PMID: WOS:000084314100001.

895 14. Bentley GN, Jones AK, Agnew A. Mapping and sequencing of acetylcholinesterase
896 genes from the platyhelminth blood fluke *Schistosoma*. Gene. 2003;314:103-12. doi:
897 10.1016/s0378-1119(03)00709-1. PubMed PMID: WOS:000186113200010.

bioRxiv preprint doi: https://doi.org/10.1101/583658; this version posted March 21, 2019. The copyright holder for this preprint (which was not certified by peer review) is the author/funder, who has granted bioRxiv a license to display the preprint in perpetuity. It is made available under aCC-BY-NC-ND 4.0 International license.

15. Bentley GN, Jones AK, Agnew A. Expression and comparative functional characterisation of recombinant acetyl cholinesterase from three species of *Schistosoma*. Molecular and Biochemical Parasitology. 2005;141(1):119-23. doi: 10.1016/j.molbiopara.2005.01.019. PubMed PMID: WOS:000228680600013.

16. You H, Gobert GN, Du X, Pali G, Cai P, Jones MK, et al. Functional characterisation of *Schistosoma japonicum* acetylcholinesterase. Parasites & Vectors. 2016;9:328. doi: 10.1186/s13071-016-1615-1. PubMed PMID: PMC4901427.

17. Berriman M, Haas BJ, LoVerde PT, Wilson RA, Dillon GP, Cerqueira GC, et al. The genome of the blood fluke *Schistosoma mansoni*. Nature. 2009;460(7253):352-8. doi: http://www.nature.com/nature/journal/v460/n7253/suppinfo/nature08160_S1.html.

18. Paraoanu LE, Layer PG. Acetylcholinesterase in cell adhesion, neurite growth and network formation. Febs j. 2008;275(4):618-24. Epub 2008/01/22. doi: 10.1111/j.1742-4658.2007.06237.x. PubMed PMID: 18205832.

19. Zhang X-J, Greenberg DS. Acetylcholinesterase involvement in apoptosis. Frontiers in Genetics. 2012;5. doi: 10.3389/fnmol.2012.00040.

20. Espinoza B, Tarrab-Hazdai R, Himmeloch S, Arnon R. Acetylcholinesterase from *Schistosoma mansoni*: immunological characterization. Immunology letters. 1991;28(2):167-74. doi: 10.1016/0165-2478(91)90116-R.

21. Jones AK, Bentley GN, Parra WGO, Agnew A. Molecular characterization of an acetylcholinesterase implicated in the regulation of glucose scavenging by the parasite Schistosoma. FASEB Journal. 2002;16(1):441-. doi: 10.1096/fj.01-0683fje.

22. Camacho M, Agnew A. *Schistosoma*: Rate of glucose import is altered by acetylcholine interaction with tegumental acetylcholine receptors and acetylcholinesterase. Experimental Parasitology. 1995;81(4):584-91. doi: 10.1006/expr.1995.1152. PubMed PMID: WOS:A1995TN32400019.

23. Sundaraneedi MK, Tedla BA, Eichenberger RM, Becker L, Pickering D, Smout MJ, et al. Polypyridylruthenium(II) complexes exert anti-schistosome activity and inhibit parasite acetylcholinesterases. PLoS neglected tropical diseases. 2017;11(12):e0006134. Epub 2017/12/15. doi: 10.1371/journal.pntd.0006134. PubMed PMID: 29240773; PubMed Central PMCID: PMCPMC5746282.

24. You H, Liu C, Du X, Nawaratna S, Rivera V, Harvie M, et al. Suppression of *Schistosoma japonicum* acetylcholinesterase affects parasite growth and development. International Journal of Molecular Sciences. 2018;19(8):2426. PubMed PMID: doi:10.3390/ijms19082426.

25. Camacho M, Alsford S, Jones A, Agnew A. Nicotinic acetylcholine receptors on the surface of the blood fluke *Schistosoma*. Molecular and biochemical parasitology. 1995;71(1):127-34. Epub 1995/04/01. PubMed PMID: 7630376.

bioRxiv preprint doi: https://doi.org/10.1101/583658; this version posted March 21, 2019. The copyright holder for this preprint (which was not certified by peer review) is the author/funder, who has granted bioRxiv a license to display the preprint in perpetuity. It is made available under aCC-BY-NC-ND 4.0 International license.

935 26. Skelly PJ, Da'dara AA, Li X-H, Castro-Borges W, Wilson RA. Schistosome Feeding
936 and Regurgitation. PLoS Pathogens. 2014;10(8):e1004246. doi:
937 10.1371/journal.ppat.1004246. PubMed PMID: PMC4133383.

938 27. Hussein AS, Harel M, Selkirk ME. A distinct family of acetylcholinesterases is secreted
939 by Nippostrongylus brasiliensis. Molecular and Biochemical Parasitology. 2002;123(2):125-
940 34. PubMed PMID: WOS:000178735800005.

941 28. Lawrence CE, Pritchard DI. Differential secretion of acetylcholinesterase and proteases
942 during the development of Heligmosomoides polygyrus. Int J Parasitol. 1993;23(3):309-14.
943 Epub 1993/05/01. PubMed PMID: 8359979.

944 29. Rathaur S, Robertson BD, Selkirk ME, Maizels RM. Secretory acetylcholinesterases
945 from Brugia malayi adult and microfilarial parasites. Mol Biochem Parasitol. 1987;26(3):257-
946 65. Epub 1987/12/01. PubMed PMID: 3123928.

947 30. Selkirk ME, Lazari O, Hussein AS, Matthews JB. Nematode acetylcholinesterases are
948 encoded by multiple genes and perform non-overlapping functions. Chemico-Biological
949 Interactions. 2005;157:263-8. doi: 10.1016/j.cbi.2005.10.039. PubMed PMID:
950 WOS:000234337000036.

951 31. Vaux R, Schnoeller C, Berkachy R, Roberts LB, Hagen J, Gounaris K, et al. Modulation
952 of the Immune Response by Nematode Secreted Acetylcholinesterase Revealed by
953 Heterologous Expression in *Trypanosoma musculi*. PLoS Pathog. 2016;12(11):e1005998.
954 Epub 2016/11/02. doi: 10.1371/journal.ppat.1005998. PubMed PMID: 27802350; PubMed
955 Central PMCID: PMCPMC5089771.

956 32. Dvir H, Silman I, Harel M, Rosenberry TL, Sussman JL. Acetylcholinesterase: from
957 3D structure to function. Chem Biol Interact. 2010;187(1-3):10-22. Epub 2010/02/09. doi:
958 10.1016/j.cbi.2010.01.042. PubMed PMID: 20138030; PubMed Central PMCID:
959 PMCPmc2894301.

960 33. Bueding E. Acetylcholinesterase activity of *Schistosoma mansoni*. British journal of
961 pharmacology and chemotherapy. 1952;7(4):563-6. PubMed PMID: MEDLINE:13019023.

962 34. Basch PF. Why do schistosomes have separate sexes? Parasitol Today. 1990;6(5):160-
963 3. Epub 1990/05/01. PubMed PMID: 15463329.

964 35. Mack A, Robitzki A. The key role of butyrylcholinesterase during neurogenesis and
965 neural disorders: an antisense-5'butyrylcholinesterase-DNA study. Prog Neurobiol.
966 2000;60(6):607-28. Epub 2000/03/30. PubMed PMID: 10739090.

967 36. Parker-Manuel SJ, Ivens AC, Dillon GP, Wilson RA. Gene Expression Patterns in
968 Larval *Schistosoma mansoni* Associated with Infection of the Mammalian Host. PLOS
969 Neglected Tropical Diseases. 2011;5(8):e1274. doi: 10.1371/journal.pntd.0001274.

bioRxiv preprint doi: https://doi.org/10.1101/583658; this version posted March 21, 2019. The copyright holder for this preprint (which was not certified by peer review) is the author/funder, who has granted bioRxiv a license to display the preprint in perpetuity. It is made available under aCC-BY-NC-ND 4.0 International license.

970 37. Gobert GN, Chai M, McManus DP. Biology of the schistosome lung-stage
971 schistosomulum. Parasitology. 2007;134(Pt 4):453-60. doi: 10.1017/S0031182006001648.
972 PubMed PMID: PMC2754249.

973 38. Arnon R, Espinoza-Ortega B, Tarrab-Hazdai R. Acetylcholinesterase of *Schistosoma*
974 *mansoni*: an antigen of functional implications. Memórias do Instituto Oswaldo Cruz.
975 1987;82:163-70.

976 39. Camacho M, Tarrab-Hazdai R, Espinoza B, Arnon R, Agnew A. The amount of
977 acetylcholinesterase on the parasite surface reflects the differential sensitivity of schistosome
978 species to metrifonate. Parasitology. 1994;108 (Pt 2):153-60. Epub 1994/02/01. PubMed
979 PMID: 8159460.

980 40. Mackintosh C. Dynamic interactions between 14-3-3 proteins and phosphoproteins
981 regulate diverse cellular processes. Biochemical Journal. 2004;381(Pt 2):329-42. doi:
982 10.1042/BJ20031332. PubMed PMID: PMC1133837.

983 41. Lee DL. Why do some nematode parasites of alimentary tract secrete
984 acetylcholinesterase? International Journal for Parasitology. 1996;26(5):499-508. doi:
985 10.1016/0020-7519(96)00040-9. PubMed PMID: WOS:A1996UW68100004.

986 42. Lee DL. The fine structure of the excretory system in adult *Nippostrongylus brasiliensis*
987 (Nematoda) and a suggested function for the 'excretory glands'. Tissue & cell. 1970;2(2):225-
988 31. Epub 1970/01/01. PubMed PMID: 18631510.

989 43. Mesulam MM, Guillozet A, Shaw P, Levey A, Duysen EG, Lockridge O.
990 Acetylcholinesterase knockouts establish central cholinergic pathways and can use
991 butyrylcholinesterase to hydrolyze acetylcholine. Neuroscience. 2002;110(4):627-39. Epub
992 2002/04/06. PubMed PMID: 11934471.

993 44. Li B, Stribley JA, Ticu A, Xie W, Schopfer LM, Hammond P, et al. Abundant tissue
994 butyrylcholinesterase and its possible function in the acetylcholinesterase knockout mouse.
995 Journal of neurochemistry. 2000;75(3):1320-31. Epub 2000/08/11. PubMed PMID: 10936216.

996 45. Greenspan RJ, Finn JA, Jr., Hall JC. Acetylcholinesterase mutants in *Drosophila* and
997 their effects on the structure and function of the central nervous system. The Journal of
998 comparative neurology. 1980;189(4):741-74. Epub 1980/02/15. doi: 10.1002/cne.901890409.
999 PubMed PMID: 6769980.

1000 46. Xie W, Stribley JA, Chatonnet A, Wilder PJ, Rizzino A, McComb RD, et al. Postnatal
1001 developmental delay and supersensitivity to organophosphate in gene-targeted mice lacking
1002 acetylcholinesterase. The Journal of pharmacology and experimental therapeutics.
1003 2000;293(3):896-902. Epub 2000/06/28. PubMed PMID: 10869390.

1004 47. Smith H, Doenhoff M, Aitken C, Bailey W, Ji M, Dawson E, et al. Comparison of
1005 *Schistosoma mansoni* soluble cercarial antigens and soluble egg antigens for serodiagnosing

bioRxiv preprint doi: https://doi.org/10.1101/583658; this version posted March 21, 2019. The copyright holder for this preprint (which was not certified by peer review) is the author/funder, who has granted bioRxiv a license to display the preprint in perpetuity. It is made available under aCC-BY-NC-ND 4.0 International license.

schistosome infections. PLOS Neglected Tropical Diseases. 2012;6(9):e1815. doi: 10.1371/journal.pntd.0001815.

48. X.-M. H, L.-W. Y, G.-L. H, Q.-P. Y, Z.-J. H, F. L. RNA interference of ace1 and ace2 in *Chilo suppressalis* reveals their different contributions to motor ability and larval growth. Insect Molecular Biology. 2011;20(4):507-18. doi: doi:10.1111/j.1365-2583.2011.01081.x.

49. Lu Y, Park Y, Gao X, Zhang X, Yao J, Pang Y-P, et al. Cholinergic and non-cholinergic functions of two acetylcholinesterase genes revealed by gene-silencing in *Tribolium castaneum*. Scientific Reports. 2012;2:288. doi: 10.1038/srep00288. PubMed PMID: PMC3286809.

50. Hussein AS, Kichenin K, Selkirk ME. Suppression of secreted acetylcholinesterase expression in *Nippostrongylus brasiliensis* by RNA interference. Molecular and Biochemical Parasitology. 2002;122(1):91-4. doi: 10.1016/s0166-6851(02)00068-3. PubMed PMID: WOS:000177290900009.

51. Johnson CD, Rand JB, Herman RK, Stern BD, Russell RL. The acetylcholinesterase genes of *C. elegans*: Identification of a third gene (ace-3) and mosaic mapping of a synthetic lethal phenotype. Neuron. 1988;1(2):165-73. doi: https://doi.org/10.1016/0896-6273(88)90201-2.

52. Lang GJ, Zhu KY, Zhang CX. Can acetylcholinesterase serve as a target for developing more selective insecticides? Current drug targets. 2012;13(4):495-501. Epub 2012/01/28. PubMed PMID: 22280346.

53. Bueding E, Liu CL, Rogers SH. Inhibition by metrifonate and DDVP of cholinesterases in schistosomes. British journal of pharmacology. 1972;46(3):480-7. doi: 10.1111/j.1476-5381.1972.tb08145.x.

54. Davis A, Bailey DR. Metrifonate in urinary schistosomiasis. Bulletin of the World Health Organization. 1969;41(2):209-24. Epub 1969/01/01. PubMed PMID: 5308698; PubMed Central PMCID: PMCPmc2427421.

55. Feldmeier H, Doehring E, Daffala AA, Omer AH, Dietrich M. Efficacy of metrifonate in urinary schistosomiasis: comparison of reduction of *Schistosoma haematobium* and *Schistosoma mansoni* eggs. The American journal of tropical medicine and hygiene. 1982;31(6):1188-94. Epub 1982/11/01. PubMed PMID: 6890775.

56. Sundaraneedi M, Eichenberger RM, Al-Hallaf R, Yang D, Sotillo J, Rajan S, et al. Polypyridylruthenium(II) complexes exert *in vitro* and *in vivo* nematocidal activity and show significant inhibition of parasite acetylcholinesterases. International Journal for Parasitology: Drugs and Drug Resistance. 2018;8(1):1-7. Epub 2017/12/06. doi: 10.1016/j.ijpddr.2017.11.005. PubMed PMID: 29207309; PubMed Central PMCID: PMCPMC5724747.

bioRxiv preprint doi: https://doi.org/10.1101/583658; this version posted March 21, 2019. The copyright holder for this preprint (which was not certified by peer review) is the author/funder, who has granted bioRxiv a license to display the preprint in perpetuity. It is made available under aCC-BY-NC-ND 4.0 International license.

1042 57. Pritchard DI. Why do some parasitic nematodes secrete acetylcholinesterase (AChE)?
1043 International journal for parasitology. 1993;23(5):549-50. Epub 1993/08/01. PubMed PMID:
1044 8225755.

1045 58. Felder CE, Botti SA, Lifson S, Silman I, Sussman JL. External and internal electrostatic
1046 potentials of cholinesterase models. J Mol Graph Model. 1997;15(5):318-27, 35-7. Epub
1047 1998/06/26. PubMed PMID: 9640563.

1048 59. Soreq H, Seidman S. Acetylcholinesterase — new roles for an old actor. Nature
1049 Reviews Neuroscience. 2001;2:294. doi: 10.1038/35067589.

1050 60. Bueding E, Schiller EL, Bourgeois JG. Some physiological, biochemical, and
1051 morphologic effects of tris (p-aminophenyl) carbonium salts (TAC) on *Schistosoma mansoni*.
1052 The American journal of tropical medicine and hygiene. 1967;16(4):500-15. Epub 1967/07/01.
1053 PubMed PMID: 4952150.

1054 61. Ittiprasert W, Mann VH, Karinshak SE, Coghlan A, Rinaldi G, Sankaranarayanan G, et
1055 al. Programmed genome editing of the omega-1 ribonuclease of the blood fluke, *Schistosoma*
1056 *mansoni*. bioRxiv. 2018:358424. doi: 10.1101/358424.

1057 62. McGehee DS, Krasowski MD, Fung DL, Wilson B, Gronert GA, Moss J.
1058 Cholinesterase inhibition by potato glycoalkaloids slows mivacurium metabolism.
1059 Anesthesiology. 2000;93(2):510-9. PubMed PMID: 10910502.

1060 63. Perrett S, Whitfield PJ. Atanine (3-dimethylallyl-4-methoxy-2-quinolone), an alkaloid
1061 with anthelmintic activity from the Chinese medicinal plant, Evodia rutaecarpa. Planta Med.
1062 1995;61(3):276-8. doi: 10.1055/s-2006-958073. PubMed PMID: 7617774.

1063 64. Saxena A, Sun W, Luo C, Myers TM, Koplovitz I, Lenz DE, et al. Bioscavenger for
1064 protection from toxicity of organophosphorus compounds. J Mol Neurosci. 2006;30(1-2):145-
1065 8. Epub 2006/12/29. PubMed PMID: 17192662.

1066 65. Boudinot E, Taysse L, Daulon S, Chatonnet A, Champagnat J, Foutz AS. Effects of
1067 acetylcholinesterase and butyrylcholinesterase inhibition on breathing in mice adapted or not
1068 to reduced acetylcholinesterase. Pharmacology biochemistry and behavior. 2005;80(1):53-61.
1069 Epub 2005/01/18. doi: 10.1016/j.pbb.2004.10.014. PubMed PMID: 15652380.

1070 66. De Vriese C, Gregoire F, Lema-Kisoka R, Waelbroeck M, Robberecht P, Delporte C.
1071 Ghrelin degradation by serum and tissue homogenates: identification of the cleavage sites.
1072 Endocrinology. 2004;145(11):4997-5005. Epub 2004/07/17. doi: 10.1210/en.2004-0569.
1073 PubMed PMID: 15256494.

1074 67. Adzhubei AA, Sternberg MJ, Makarov AA. Polyproline-II helix in proteins: structure
1075 and function. J Mol Biol. 2013;425(12):2100-32. Epub 2013/03/20. doi:
1076 10.1016/j.jmb.2013.03.018. PubMed PMID: 23507311.

bioRxiv preprint doi: https://doi.org/10.1101/583658; this version posted March 21, 2019. The copyright holder for this preprint (which was not certified by peer review) is the author/funder, who has granted bioRxiv a license to display the preprint in perpetuity. It is made available under aCC-BY-NC-ND 4.0 International license.

1077 68. Ramalho-Pinto FJ, Gazzinelli G, Howells RE, Mota-Santos TA, Figueiredo EA,
1078 Pellegrino J. *Schistosoma mansoni*: defined system for stepwise transformation of cercaria to
1079 schistosomule *in vitro*. Experimental parasitology. 1974;36(3):360-72. Epub 1974/12/01.
1080 PubMed PMID: 4139038.

1081 69. Lewis FA, Stirewalt MA, Souza CP, Gazzinelli G. Large-scale laboratory maintenance
1082 of *Schistosoma mansoni,* with observations on three schistosome/snail host combinations. The
1083 Journal of parasitology. 1986;72(6):813-29. Epub 1986/12/01. PubMed PMID: 3546654.

1084 70. Basch PF. Cultivation of *Schistosoma mansoni In vitro*. I. Establishment of cultures
1085 from cercariae and development until pairing. The Journal of parasitology. 1981;67(2):179-85.
1086 Epub 1981/04/01. PubMed PMID: 7241277.

1087 71. Sotillo J, Pearson M, Becker L, Mulvenna J, Loukas A. A quantitative proteomic
1088 analysis of the tegumental proteins from *Schistosoma mansoni* schistosomula reveals novel
1089 potential therapeutic targets. International journal for parasitology. 2015;45(8):505-16. doi:
1090 10.1016/j.ijpara.2015.03.004.

1091 72. Kumar S, Stecher G, Tamura K. MEGA7: Molecular Evolutionary Genetics Analysis
1092 Version 7.0 for Bigger Datasets. Mol Biol Evol. 2016;33(7):1870-4. Epub 2016/03/24. doi:
1093 10.1093/molbev/msw054. PubMed PMID: 27004904.

1094 73. Long T, Neitz RJ, Beasley R, Kalyanaraman C, Suzuki BM, Jacobson MP, et al.
1095 Structure-Bioactivity Relationship for Benzimidazole Thiophene Inhibitors of Polo-Like
1096 Kinase 1 (PLK1), a Potential Drug Target in Schistosoma mansoni. PLOS Neglected Tropical
1097 Diseases. 2016;10(1):e0004356. doi: 10.1371/journal.pntd.0004356.

1098 74. Schmittgen TD, Livak KJ. Analyzing real-time PCR data by the comparative C(T)
1099 method. Nat Protoc. 2008;3(6):1101-8. Epub 2008/06/13. PubMed PMID: 18546601.

1100 75. Ellman GL, Courtney KD, Andres V, Featherstone RM. A new and rapid colorimetric
1101 determination of acetylcholinesterase activity. Biochemical Pharmacology. 1961;7(2):88-95.
1102 doi: https://doi.org/10.1016/0006-2952(61)90145-9.

1103 76. Hodgson AJ, Chubb IW. A method for the detection and quantitation of secretory
1104 acetylcholinesterase. Neurochemical Pathology. 1983;1(3):211. doi: 10.1007/bf02834246.

1105 77. Tran MH, Pearson MS, Bethony JM. Tetraspanins on the surface of Schistosoma
1106 mansoni are protective antigens against schistosomiasis. Nature Medicine 2006;12(7):835.

1107 78. Wangchuk P, Giacomin PR, Pearson MS, Smout MJ, Loukas A. Identification of lead
1108 chemotherapeutic agents from medicinal plants against blood flukes and whipworms.
1109 Scientific Reports. 2016;6:32101. doi: 10.1038/srep32101.

1110

1111

bioRxiv preprint doi: https://doi.org/10.1101/583658; this version posted March 21, 2019. The copyright holder for this preprint (which was not certified by peer review) is the author/funder, who has granted bioRxiv a license to display the preprint in perpetuity. It is made available under aCC-BY-NC-ND 4.0 International license.

1112 **Figure captions**

1113 **Figure 1. The amino acid sequence alignment and phylogeny of ChEs from *S. mansoni***
1114 **and other species.** Light blue arrowheads = the 14 aromatic rings, black arrowheads =
1115 oxyanion holes, S= salt bridges, red boxes= PAS, yellow boxes = catalytic triad, green boxes
1116 = acyl binding pocket, numbered arrows = disulfide bonds and magenta box = peripheral
1117 anionic site. Accession numbers: *H. sapiens* (NP000656), *T. californica* (CAA27169), *C.*
1118 *elegans* (NP510660), *Sm*AChE1 (Smp_154600), *Sm*BChE1 (Smp_125350), *Sm*AChE3
1119 (Smp_136690).

1120

1121 **Figure 2. Developmental expression profiles of *smache1*, *smbche1* and *smache3*.** The
1122 expression of (A) *smache1*, (B) *smbche1*and (C) *smache3* genes at different developmental
1123 stages of *S. mansoni* as quantified by qPCR analysis. (D) The heat map shows the comparative
1124 expression pattern of the paralogs in each developmental stage. Data are presented as
1125 mean ± SEM of five independent experiments and are normalized to the *smcox1*
1126 housekeeping gene.

1127

1128 **Figure 3. Immunofluorescent localization of *Sm*ChEs**. Fluorescence and brightfield images
1129 of (A) male (M) and female (F) *S. mansoni* and *S. haematobium* adult worm sections. (B) Live,
1130 fixed cercariae, and schistosomula at 3 h, 24 h, 3 days and 5 days after transformation. Both
1131 adult sections and juvenile parasites were labeled with either anti-*Sm*AChE1, anti-*Sm*BChE1
1132 or anti-*Sm*AChE3 primary antibody (1:100 in PBST) followed by goat-anti-mouse IgG-
1133 alexafluor 647 (1:200 in PBST). Naive mouse sera was used as a negative control.

1134

1135 **Figure 4. Enzymatic activity of f*Sm*ChEs.** (A) Cholinergic substrate preference (AcSCh or
1136 BcSCh) of each f*Sm*ChE. (B) Inhibition of f*Sm*AChE1 and f*Sm*AChE3 with DDVP (AcSCh

bioRxiv preprint doi: https://doi.org/10.1101/583658; this version posted March 21, 2019. The copyright holder for this preprint (which was not certified by peer review) is the author/funder, who has granted bioRxiv a license to display the preprint in perpetuity. It is made available under aCC-BY-NC-ND 4.0 International license.

used as a substrate) and inhibition of f*Sm*BChE1 with iso-OMPA (BcSCh used as a substrate). Data are presented as mean ± SEM of triplicate experiments and differences between groups were measured by the student's *t* test. **P* ≤ 0.05, ***P* ≤ 0.01, ****P* ≤ 0.001.

Figure 5. BChE and secreted ChE activity in schistosomes. (A) BChE activity in *S. mansoni* adults and schistosomula TX-100 extracts. (B) BChE activity in TX-100 extracts from *S. mansoni* and S. *haematobium***.** (C) AChE and (D) BChE activity of ES products from different developmental stages of *S. mansoni*. (E) AChE activity and (F) SDS-PAGE analysis of purified, secreted *Sm*ChEs. Data are presented as mean ± SEM of triplicate experiments and differences between groups were measured by the student's *t* test. **P* ≤ 0.05, ***P* ≤ 0.01.

Figure 6. Suppression of *smche* mRNA transcript and protein expression in schistosomula by RNAi. Individual siRNA treatment with (A) *smache1*, (B) *smbche1* or (C) *smache3* siRNAs. (D) Treatment with a cocktail of *smache1*, *smbche1* and *smache3* siRNAs. Transcript levels of each *smche* in parasites treated with *smche* siRNAs are shown relative to *smche* transcript expression in schistosomula treated with the *luc* control siRNA (dashed line) and represent the mean ± SEM of triplicate qPCR assays from 2 biological replicates of each treatment. Transcript expression in all parasites was normalized with the housekeeping gene, *smcox1*. Differences in transcript levels (relative to the *luc* control) were measured by the student's *t* test. **P* ≤ 0.05, ***P* ≤ 0.01, ****P* ≤ 0.001. (E) Western blot of day 7 schistosomula extracts following treatment with *smche* or *luc* siRNAs**.** Extracts were immunoblotted with the corresponding anti-*Sm*AChE1, anti-*Sm*BChE or anti-*Sm*AChE3 polyclonal antibody. An antibody against *Sm*Pmy (paramyosin) was used as a loading control.

bioRxiv preprint doi: https://doi.org/10.1101/583658; this version posted March 21, 2019. The copyright holder for this preprint (which was not certified by peer review) is the author/funder, who has granted bioRxiv a license to display the preprint in perpetuity. It is made available under aCC-BY-NC-ND 4.0 International license.

Figure 7. Effects of *smche* knockdown on cholinesterase activity and glucose uptake. (A) AChE activity of extracts from schistosomula treated with *smache1*, *smache3* or *luc* siRNAs (dashed line). (B) BChE activity of extracts from schistosomula treated with *smbche1* or *luc* siRNAs (dashed line). (C) AChE activity of extracts from schistosomula treated with all 3 siRNAs or *luc* siRNA (dashed line). (D) Glucose uptake by schistosomula 48 h after treatment with *smche* siRNAs. Schistosomula (5 days old – 5,000/treatment) were electroporated with either *luc* or *smche* siRNAs and glucose consumption was measured 48 h after treatment. Data represents mean ± SEM of duplicate assays from 2 biological replicates of each treatment. Differences (relative to the *luc* control) were measured by the student's *t* test. $^{**}P \leq 0.01$, $^{***}P \leq 0.001$.

Figure 8. Effects of *smche* silencing on schistosomula viability *in vitro* and development *in vivo*. (A) Schistosomula treated with individual or a cocktail of all 3 *smche* siRNAs or *luc* siRNA were cultured for 7 days in complete Basch medium with viability determined at day 1, 3, 5 and 7 after treatment by Trypan Blue exclusion (mean ± SEM of duplicate assays from 2 biological replicates of each treatment). (B and C) One-day-old schistosomula treated with individual or a cocktail of all three *smche* siRNAs or *luc* siRNA were intramuscularly injected (2,000 parasites) into mice. After 3 weeks, adult worms were recovered and counted. Data from two independent experiments are shown. Differences between *smche*- and *luc*-treated groups were measured by the student's *t* test. $^{*}P \leq 0.05$, $^{**}P \leq 0.01$, $^{***}P \leq 0.001$.

Figure 9. *Sm*BChE1 bio-scavenges DDVP and protects parasites against DDVP-induced effects. (A) Schistosomula extracts were treated with DDVP (1 μM), or pretreated with iso-OMPA (1 and 2 mM) and then DDVP, before assaying AChE activity. (B) Schistosomula were treated with DDVP (1 μM) or pretreated with iso-OMPA (100 μM) and then DDVP, and

bioRxiv preprint doi: https://doi.org/10.1101/583658; this version posted March 21, 2019. The copyright holder for this preprint (which was not certified by peer review) is the author/funder, who has granted bioRxiv a license to display the preprint in perpetuity. It is made available under aCC-BY-NC-ND 4.0 International license.

parasite viability was measured 5 h after treatment. (C) *smbche1*-silenced or *luc* siRNA-treated schistosomula were treated with DDVP (1 μM) and parasite viability was measured 5 h after treatment. (D) Schistosomula extracts were pre-incubated with f*Sm*BChE1 (10 μg) then treated with DDVP (1 μM), or treated with DDVP alone, before assaying AChE activity. (E) DDVP was pre-incubated with f*Sm*BChE1 (10, 5 and 2.5 μg) or 10 μg of *Sm*TSP2 for 1 h before being used to treat schistosomula. Parasite viability was measured 24 h post-treatment. For all assays, data are the average of triplicate biological and technical experiments ± SEM and differences were measured by the student's *t* test. *$P \leq 0.05$, ***$P \leq 0.001$, ****$P \leq 0.0001$.

Supporting information

Figure S1. Regional amino acid sequence alignment of SmBChE1 and its human and other helminth homologs. Accession numbers: *Schistosoma mansoni* (*Sm*BChE1 – Smp_125350), *Schistosoma rodhaini* (SROB_0000329201), *Schistosoma haematobium* (KGB33101), *Schistosoma japonicum* (Sjp_0015690), *Clonorchis sinensis (*csin111679), *Echinostoma caproni* (ECPE_0000670801), *Fasciola hepatica* (PIS83327.1), *Hymenolepis diminuta* (HDID_0000005301), *Echinococcus granulosus* (EGR_07475.1), *Taenia solium* (TsM_000234300), *Taenia saginata* (TSAs00071g07627m00001), *Trichuris muris* (TMUE_3000012587), *Trichuris trichiura* (TTRE_0000364501), *Trichuris suis (*M514_03850), *Nippostrongylus brasiliensis* (NBR_0000102801), *Caenorhabditis elegans* (Y48B6A.8.1). Red box = catalytic triad residue.

Figure S2. Magnified view of 3D models showing the catalytic triads of *Sm*AChE1, *Sm*BChE1, and *Sm*AChE3. The amino acid residues of the catalytic triad of each paralog are

bioRxiv preprint doi: https://doi.org/10.1101/583658; this version posted March 21, 2019. The copyright holder for this preprint (which was not certified by peer review) is the author/funder, who has granted bioRxiv a license to display the preprint in perpetuity. It is made available under aCC-BY-NC-ND 4.0 International license.

magnified and their position number is given according to *Torpedo* AChE numbering: *Sm*AChE1 (Ser277, Gln538, Glu406), *Sm*BChE1 (Ser244, Gln538, Glu406), and *Sm*AChE3 (Ser239, His514, Glu375).

Figure S3. Relationship between *Sm*ChEs and other invertebrate and vertebrate species. Evolutionary history was inferred using the Neighbor-Joining method and the phylogenetic tree was generated using a ClustalW alignment. The evolutionary distances were computed using the Poisson correction method and are in the units of the number of amino acid substitutions per site. All positions containing gaps and missing data were eliminated, making for a total of 236 positions in the final dataset. The three *Sm*ChEs are indicated by bold font inside a red box. Accession numbers: *Schistosoma mansoni* (Sm_AChE1 - Smp_154600, Sm_BChE1 - Smp_125350, Sm_AChE3 - Smp_136690)*; Schistosoma bovis* (Sb_AChE1 - AAQ14323); *Schistosoma haematobium* (Sh_AChE1 - AAQ14322, Sh_AChE2 - KGB33101, Sh_AChE3 - KGB33661)*; Schistosoma japonicum* (Sj_AChE1 - ANH56887, Sj_AChE2 - Sjp0045440.1); *Clonorchis sinensis* (Cs_AChE1 - GAA52478, Cs_AChE2 - GAA53463, Cs_AChE3 - GAA27255); *Opisthorchis viverrini* (Ov_AChE - XP009170845, Ov_AChE - XP009168237, Ov_AChE - XP009170760); *Echinococcus granulosus* (Eg_AChE1 - JN662938, Eg_AChE2 - EgG000732400); *Hymenolepis microstoma* (Hm_AChE1 - LK053025); *Taenia solium* (Ts_AChE1 - TsM000234300, Ts_AChE - TsM001220100, Ts_AChE - TsM000001700); *Anopheles gambiae* (Ag_AChE1 - AGM16375); *Aedes aegypti* (Ae_AChE - AAB35001); *Culex tritaeniorhynchus* (Ct_AChE - BAD06210); *Caenorhabditis elegans* (Ce_AChE1 - NP510660, Ce_AChE2 - NP491141, Ce_AChE3 - NP496963); *Trichuris muris* (Tm_AChE1 - TMUEs0033000600); *Nippostrongylus brasiliensis* (Nb_AChE1 - AAK44221, Nb_AChE2 - AAC05785, Nb_AChE3 - AAK44221); *Homo sapiens* (Hs_AChE - NP000656); *Torpedo*

bioRxiv preprint doi: https://doi.org/10.1101/583658; this version posted March 21, 2019. The copyright holder for this preprint (which was not certified by peer review) is the author/funder, who has granted bioRxiv a license to display the preprint in perpetuity. It is made available under aCC-BY-NC-ND 4.0 International license.

californica (Tc_AChE - CAA27169); *Danio rerio* (Dr_AChE - NP571921); *Mus musculus* (Mm_AChE - CAA39867); *Rattus norvegicus* (Rn_AChE - NP742006).

Figure S4. Phylogenetic analysis of *Sm*BChE1 and its human and other helminth homologs. The phylogenetic tree was built using the maximum likelihood method with *Sm*BChE1 and the top 16 helminth ChE homologs identified from the BLASTp search, as well as human BChE. Accession numbers: *Schistosoma mansoni* (*Sm*BChE1 – Smp_125350), *Schistosoma rodhaini* (SROB_0000329201), *Schistosoma haematobium* (KGB33101), *Schistosoma japonicum* (Sjp_0015690), *Clonorchis sinensis (*csin111679), *Echinostoma caproni* (ECPE_0000670801), *Fasciola hepatica* (PIS83327.1), *Hymenolepis diminuta* (HDID_0000005301), *Echinococcus granulosus* (EGR_07475.1), *Taenia solium* (TsM_000234300), *Taenia saginata* (TSAs00071g07627m00001), *Trichuris muris* (TMUE_3000012587), *Trichuris trichiura* (TTRE_0000364501), *Trichuris suis (*M514_03850), *Nippostrongylus brasiliensis* (NBR_0000102801), *Caenorhabditis elegans* (Y48B6A.8.1).

Figure S5. Transcript levels of glucose transporters *sgtp1* and *sgtp4* and each *smche* in individual and cocktail *smche* siRNA-treated schistosomula. Transcript levels of each *smche* and *sgtp* in parasites treated with *smche* siRNAs are shown relative to *smche* transcript expression in schistosomula treated with the *luc* control siRNA (dashed line) and represent the mean ± SEM of triplicate qPCR assays from 2 biological replicates of each treatment). Transcript expression in all parasites was normalized with the housekeeping gene, *smcox1*. Differences in transcript levels (relative to the *luc* control) were measured by the student's *t* test. $*P \leq 0.05$, $**P \leq 0.01$, $***P \leq 0.001$.

bioRxiv preprint doi: https://doi.org/10.1101/583658; this version posted March 21, 2019. The copyright holder for this preprint (which was not certified by peer review) is the author/funder, who has granted bioRxiv a license to display the preprint in perpetuity. It is made available under aCC-BY-NC-ND 4.0 International license.

1257 **Table S1. Primers used in this study**

Gene	Direction	Primer Sequence
Full-length ORF expression in P. pastoris		
fsmache1	Fwd	GAATTCGCGGCCGCGAATTC
	Rev	TCTAGAGGTCTAGAGCTCGAG
fsmbche1	Fwd	GAATTCGCGGCCGCGAATTC
	Rev	TCTAGAGGTCTAGAGCTCGAG
fsmache3	Fwd	GAATTCGCGGCCGCGAATTC
	Rev	TCTAGAGGTCTAGAGCTCGAG
Partial ORF expression in E. coli		
rsmache1	Fwd	GACAGAAACCACATGATGTTGGAA
	Rev	TTCCAACATCATGTGGTTTCTGTC
rsmbche1	Fwd	TCCAGGAAGCACATGGTCTTCACT
	Rev	AGTGAAGACCATGTGCTTCCTGGA
rsmache3	Fwd	CGCCATATGCTCTCCAAAGCGTGGTTACT
	Rev	CGCCTCGAGCGGATCCCAACTTAGTCTCATC
qPCR		
smache1	Fwd	ATGGATATGAGATTGAGTATG
	Rev	CTGGAAGGATGTTAGGAT
smbche1	Fwd	CTACTCGTAATGATGACT
	Rev	GGCTGAATTATACAAGATT
smache3	Fwd	ATGCGACCACACTATCACCA
	Rev	CCTGATGTAAATCCACCACCA
sgtp1	Fwd	CTGCAGCTTATTCACTGAGTCAATC
	Rev	CCACCGATGTTTTTCTGTATAACAGGAT
sgtp4	Fwd	AGCCAAGGAGTTAACTTATTATGCAATTTATTG
	Rev	TCCAACAGATAATAACGATAACTAAAAATGGTAAGAA
smcox1	Fwd	TAGGGTTGGTGGTGTCACAG
	Rev	ACGGCCATCACCATACTAGC

1258

1259

1260

1261

bioRxiv preprint doi: https://doi.org/10.1101/583658; this version posted March 21, 2019. The copyright holder for this preprint (which was not certified by peer review) is the author/funder, who has granted bioRxiv a license to display the preprint in perpetuity. It is made available under aCC-BY-NC-ND 4.0 International license.

Table S2. Target sequences used to design siRNA duplexes

Gene	Target sequence for siRNA duplex
smache1	CAGGAGCTTTAATGTTTGGCA
smbche1	GTATCATCTTGTACAAAGTTTAAGA
smache3	CATCAAAACCAATTGGTAAATTACGT
luc	ACTGAGACTACATCAGCTATTCTGAT

Table S3. Identification by LC-MS/MS of *Sm*ChEs purified from adult *S. mansoni* ES products

Accession number[a]	Score	Seq(Sig)[b]	emPAI[c]	Protein sequences
Smp_154600.1 (*Sm*AChE1)	15457	19	4.64	SFKCPTINMATAVTNDYR CPTINMATAVTNDYR RAHTLPVYFYEFQHR AHTLPVYFYEFQHR TVSLPMPK QLSDIMMTYWANFAR TGDPNILPDGR HVTDNLNPDDPDEITEDQLK NPFIGWPEFR NPFIGWPEFRNSTK SAPANLLVSTRPR RWYPALLQQVER
Smp_125350.1 (*Sm*BChE1)	89	2	0.18	ALGTGSWTSLEVVK YETYSPHSVATR

[a] identified from Uniprot database.
[b] number of significant, distinct sequences
[c] exponentially modified protein abundance index

bioRxiv preprint doi: https://doi.org/10.1101/583658; this version posted March 21, 2019. The copyright holder for this preprint (which was not certified by peer review) is the author/funder, who has granted bioRxiv a license to display the preprint in perpetuity. It is made available under aCC-BY-NC-ND 4.0 International license.

Figure 1

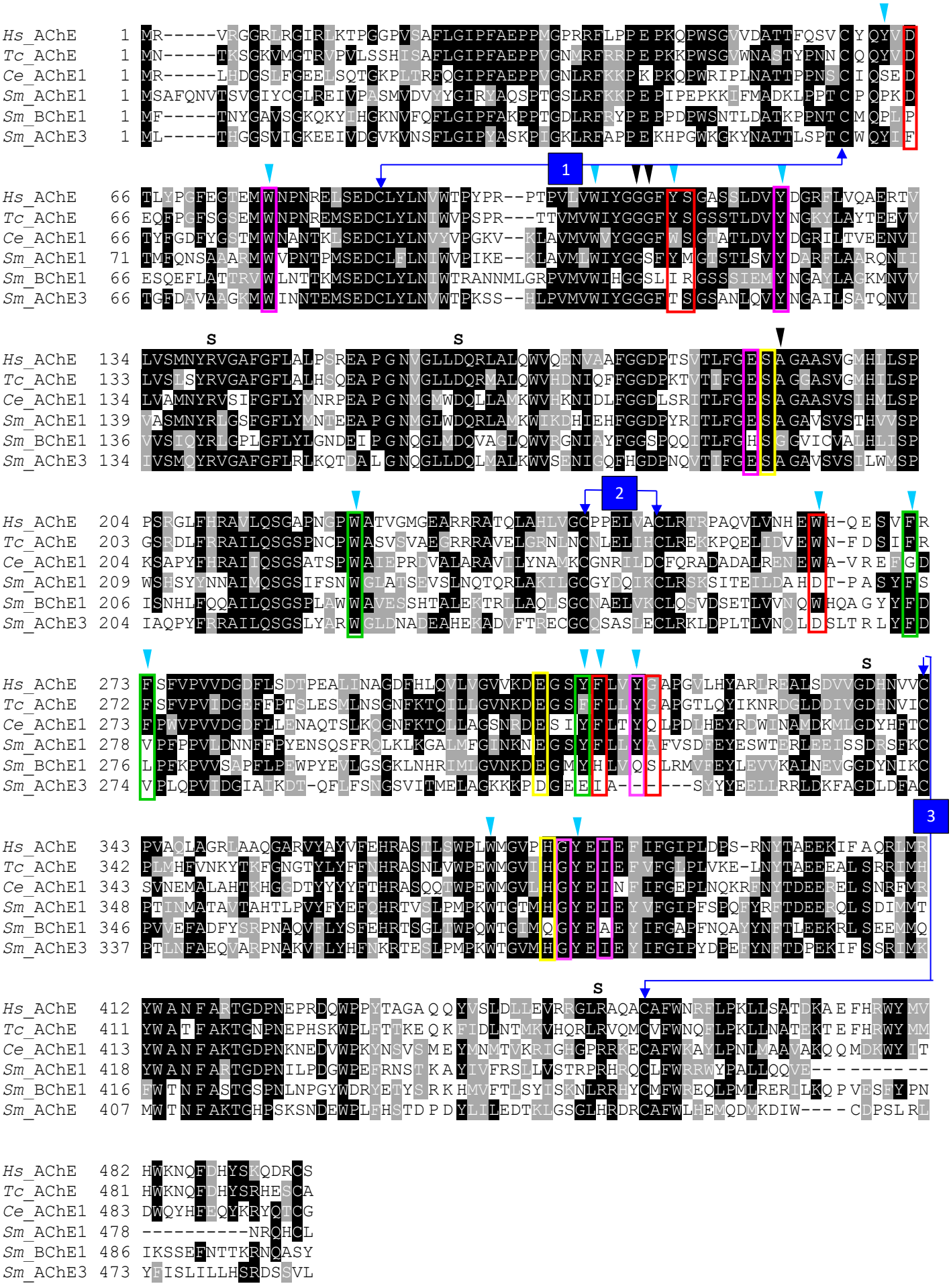

Figure 2

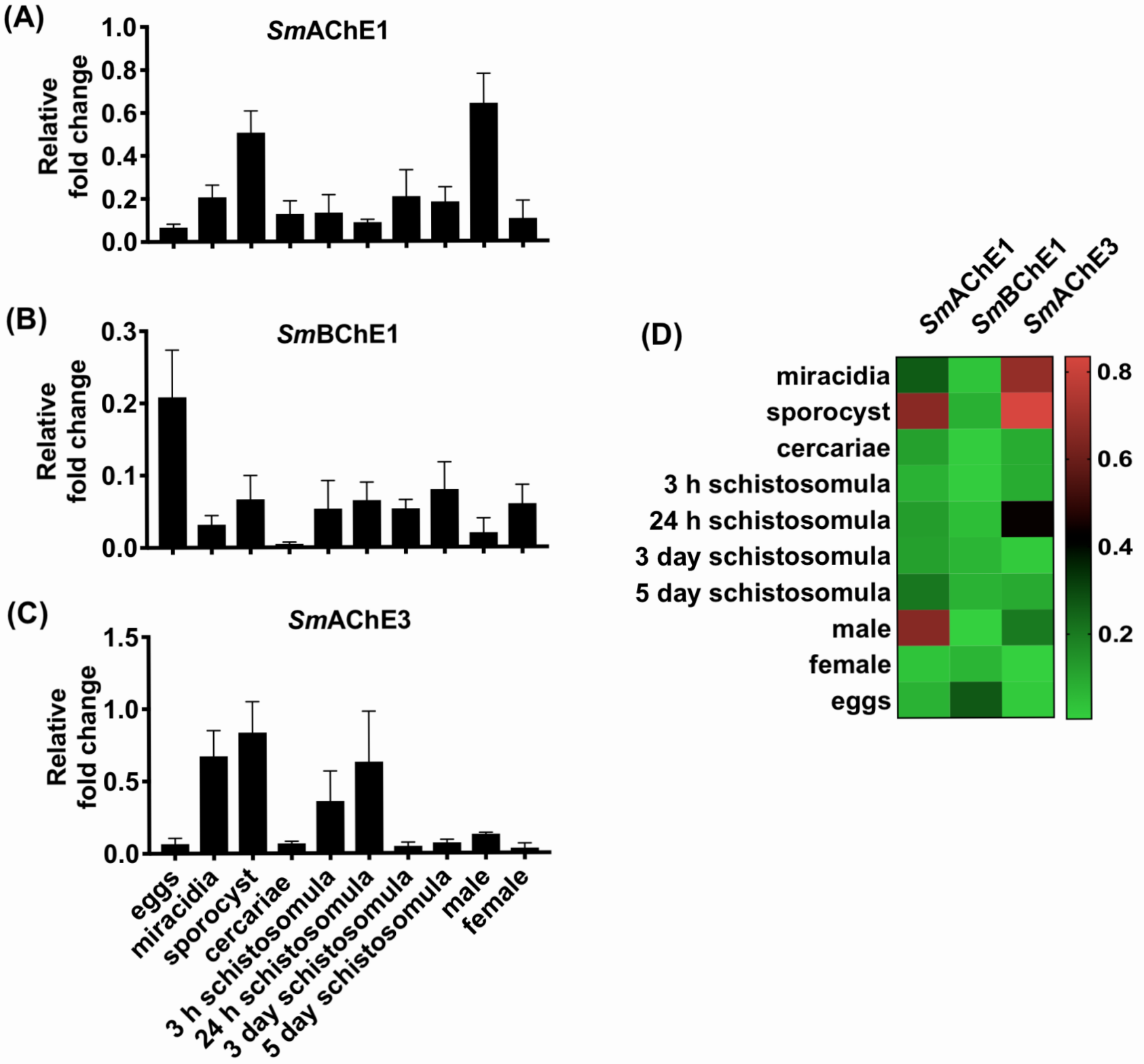

bioRxiv preprint doi: https://doi.org/10.1101/583658; this version posted March 21, 2019. The copyright holder for this preprint (which was not certified by peer review) is the author/funder, who has granted bioRxiv a license to display the preprint in perpetuity. It is made available under aCC-BY-NC-ND 4.0 International license.

figure 3

bioRxiv preprint doi: https://doi.org/10.1101/583658; this version posted March 21, 2019. The copyright holder for this preprint (which was not certified by peer review) is the author/funder, who has granted bioRxiv a license to display the preprint in perpetuity. It is made available under aCC-BY-NC-ND 4.0 International license.

figure 4

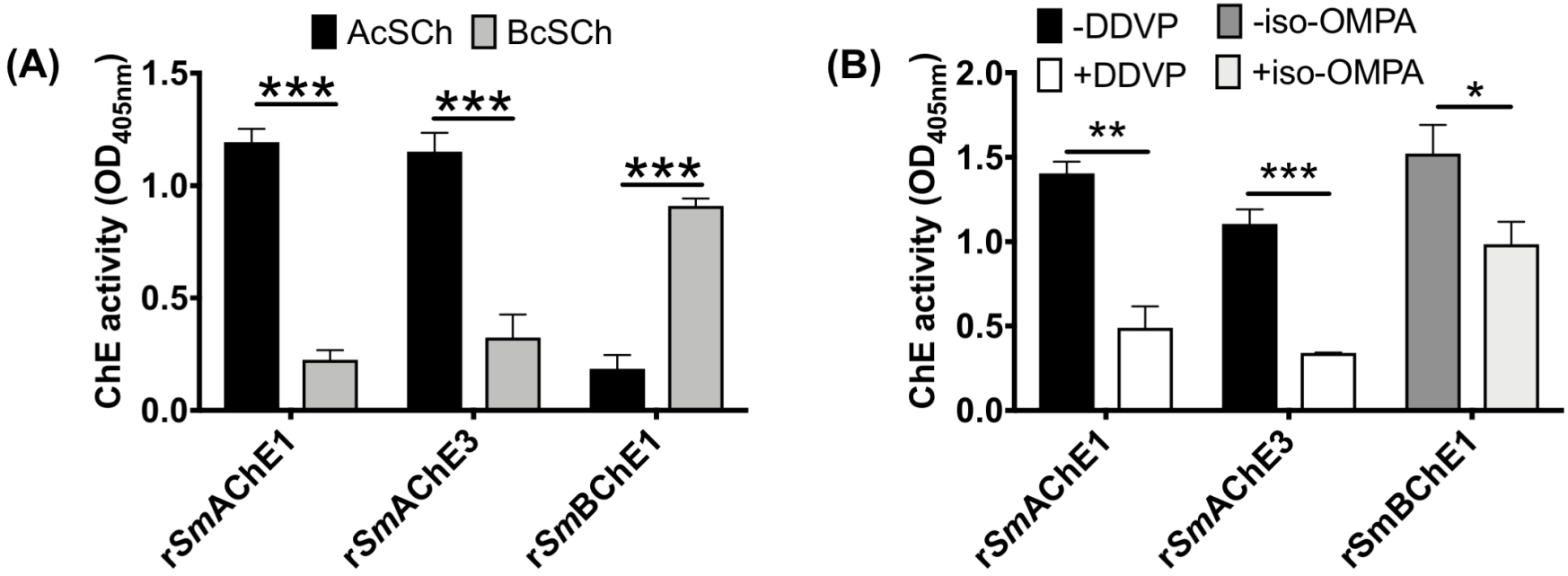

bioRxiv preprint doi: https://doi.org/10.1101/583658; this version posted March 21, 2019. The copyright holder for this preprint (which was not certified by peer review) is the author/funder, who has granted bioRxiv a license to display the preprint in perpetuity. It is made available under aCC-BY-NC-ND 4.0 International license.

figure 5

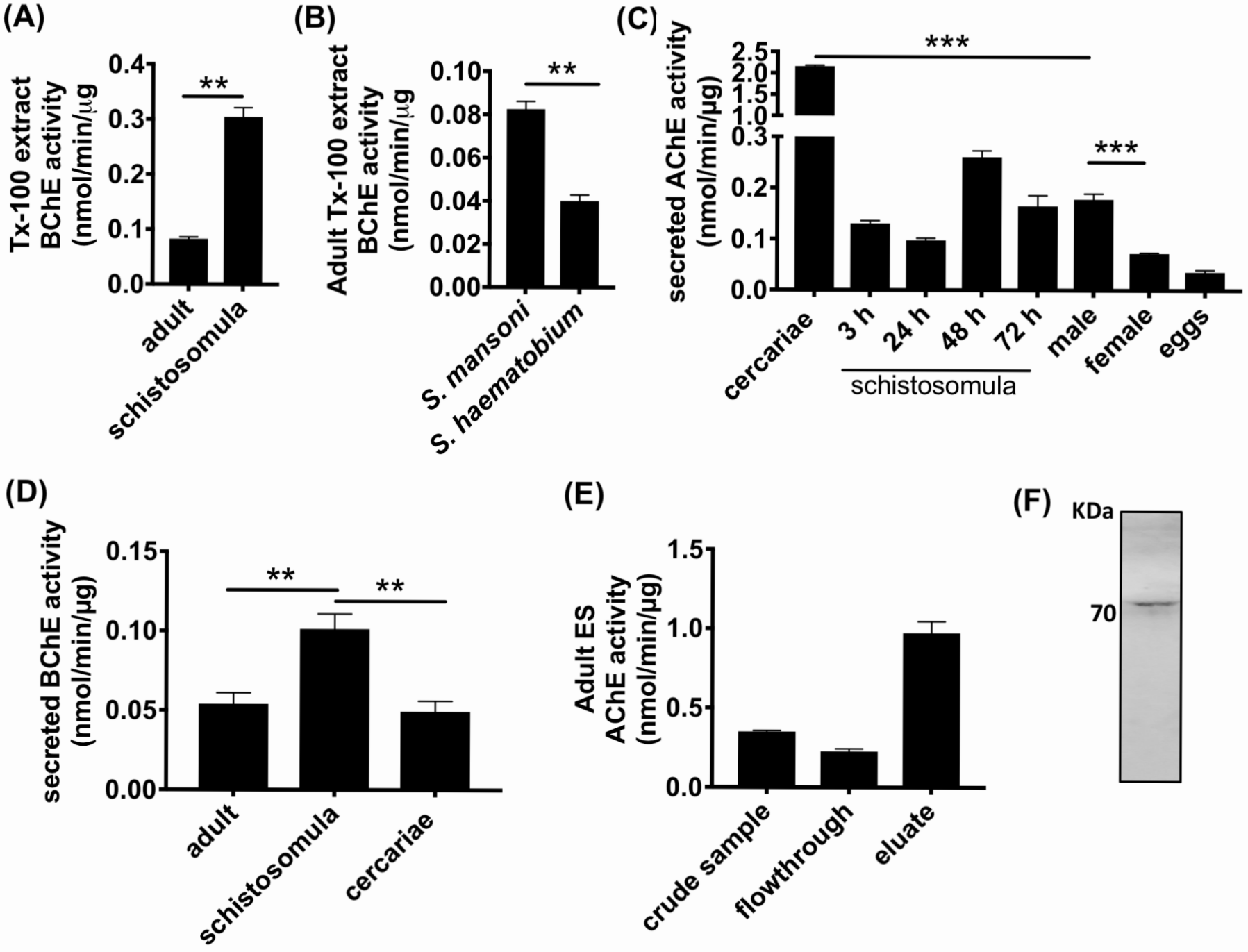

bioRxiv preprint doi: https://doi.org/10.1101/583658; this version posted March 21, 2019. The copyright holder for this preprint (which was not certified by peer review) is the author/funder, who has granted bioRxiv a license to display the preprint in perpetuity. It is made available under aCC-BY-NC-ND 4.0 International license.

figure 6

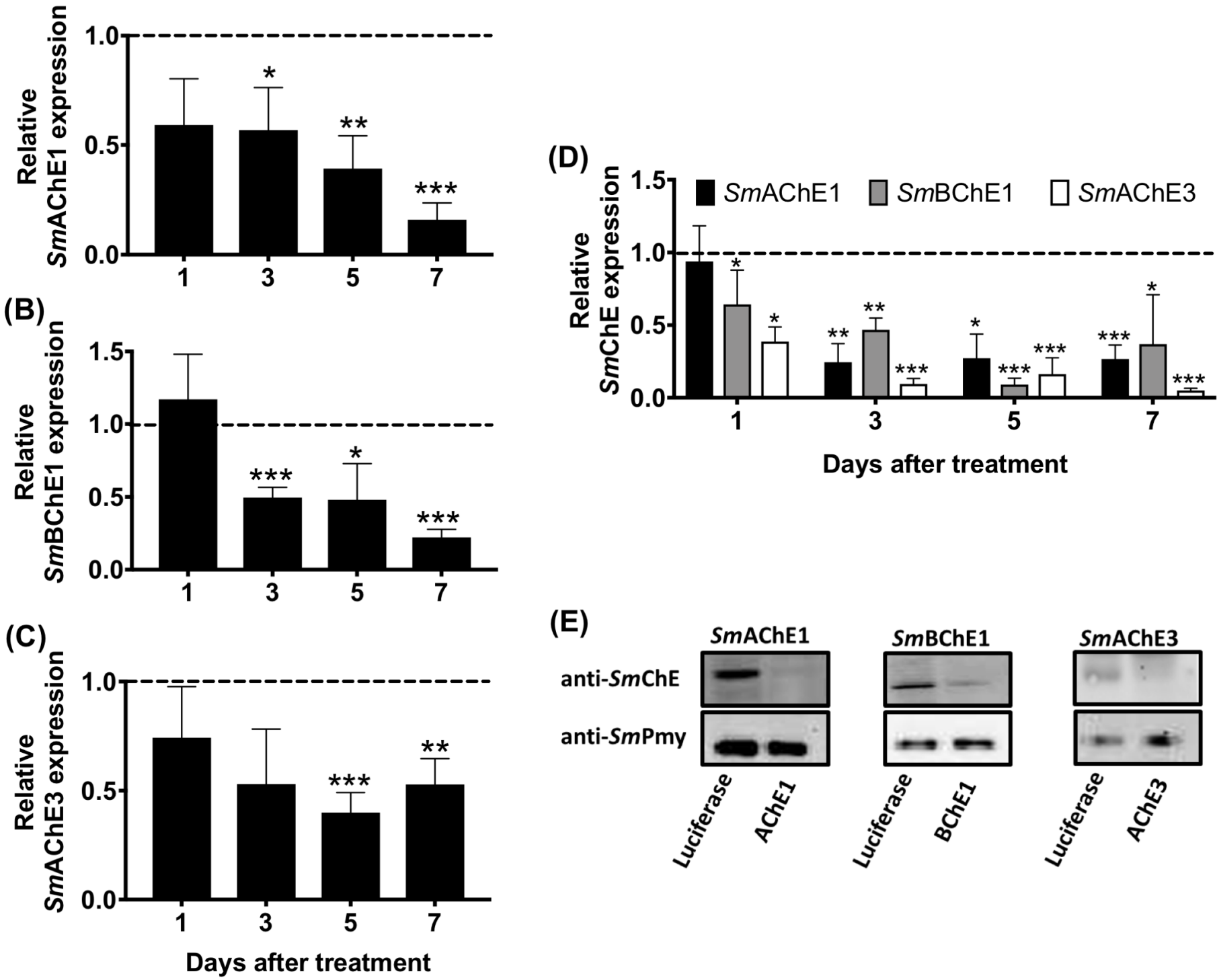

bioRxiv preprint doi: https://doi.org/10.1101/583658; this version posted March 21, 2019. The copyright holder for this preprint (which was not certified by peer review) is the author/funder, who has granted bioRxiv a license to display the preprint in perpetuity. It is made available under aCC-BY-NC-ND 4.0 International license.

figure 7

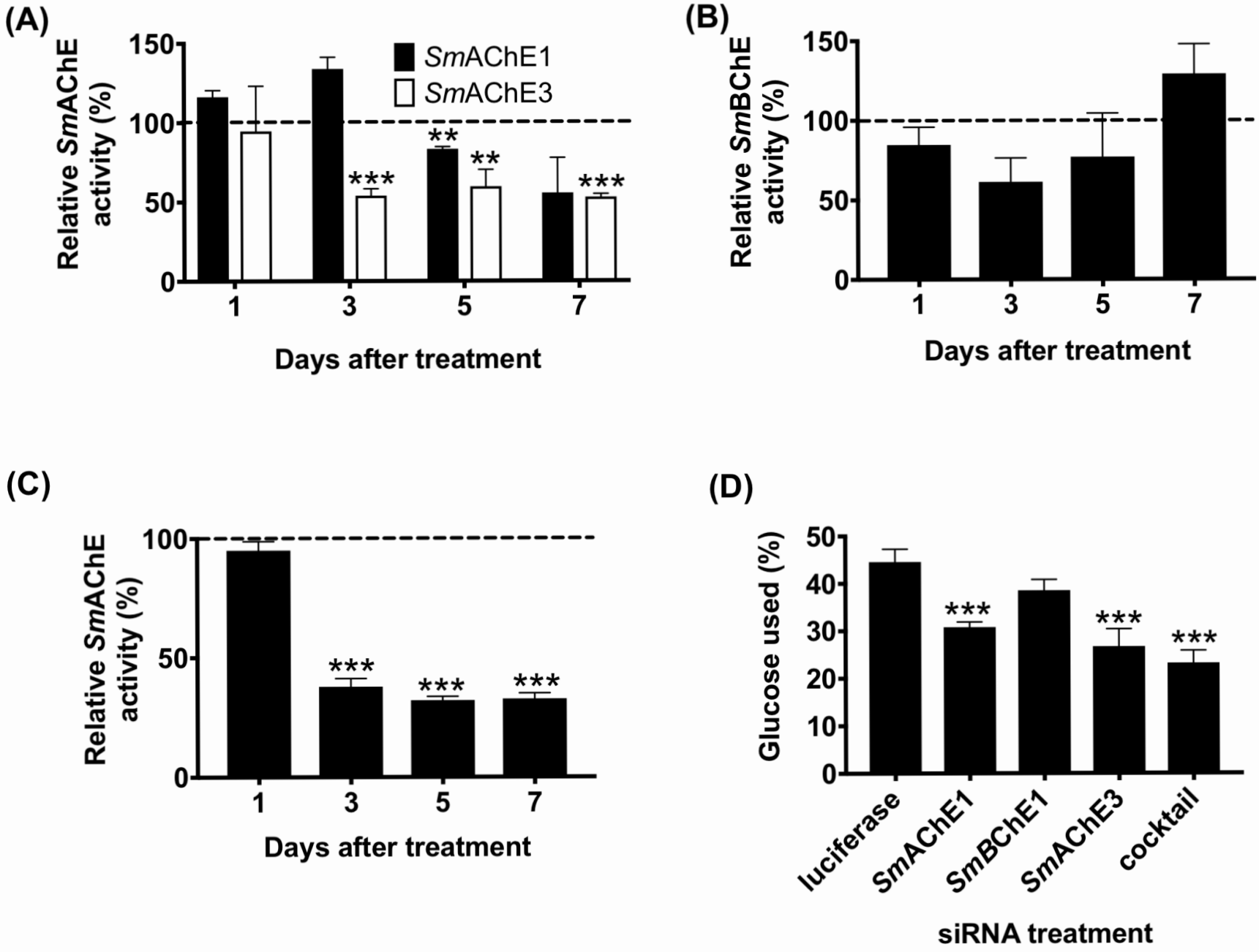

bioRxiv preprint doi: https://doi.org/10.1101/583658; this version posted March 21, 2019. The copyright holder for this preprint (which was not certified by peer review) is the author/funder, who has granted bioRxiv a license to display the preprint in perpetuity. It is made available under aCC-BY-NC-ND 4.0 International license.

figure 8

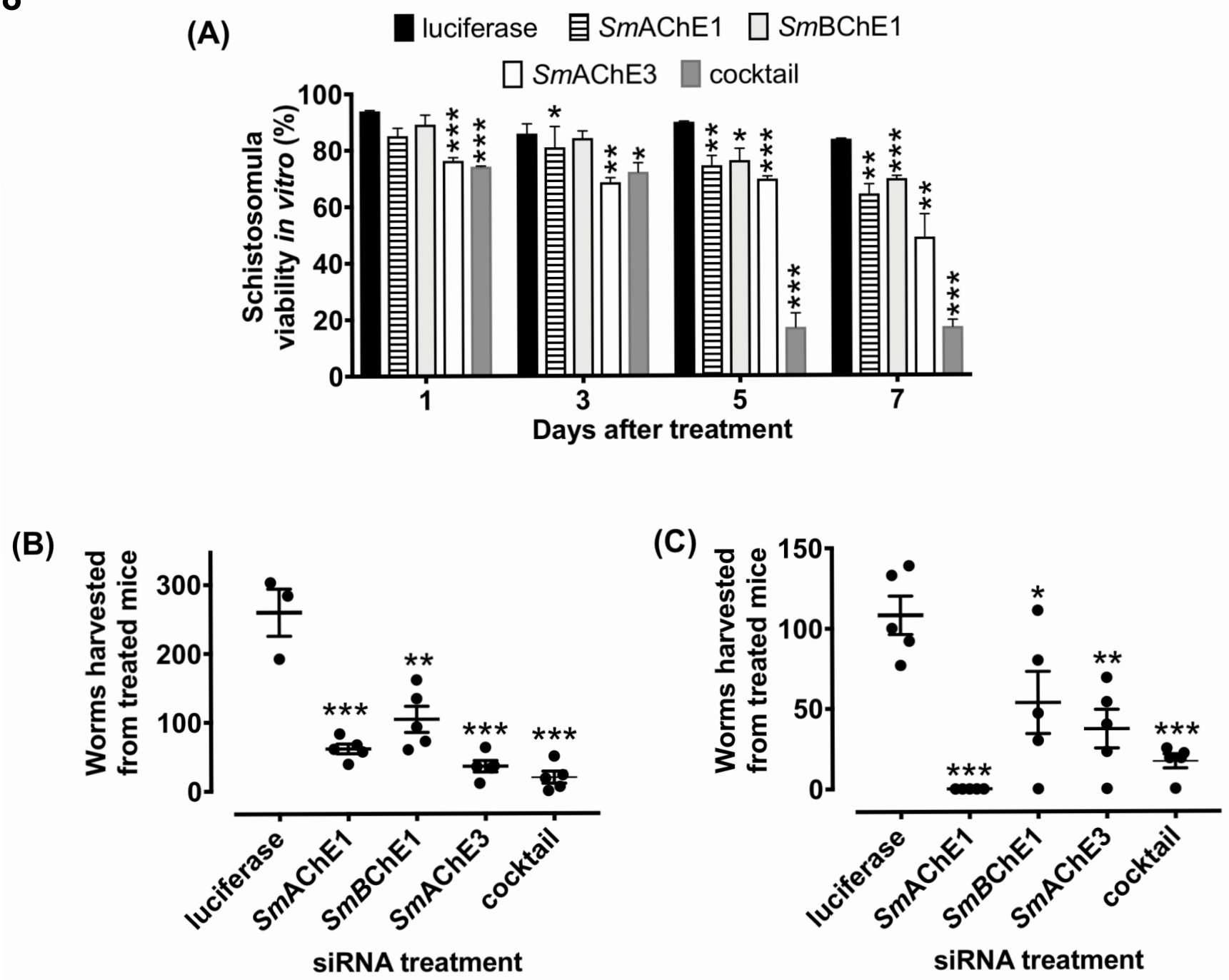

bioRxiv preprint doi: https://doi.org/10.1101/583658; this version posted March 21, 2019. The copyright holder for this preprint (which was not certified by peer review) is the author/funder, who has granted bioRxiv a license to display the preprint in perpetuity. It is made available under aCC-BY-NC-ND 4.0 International license.

figure 9

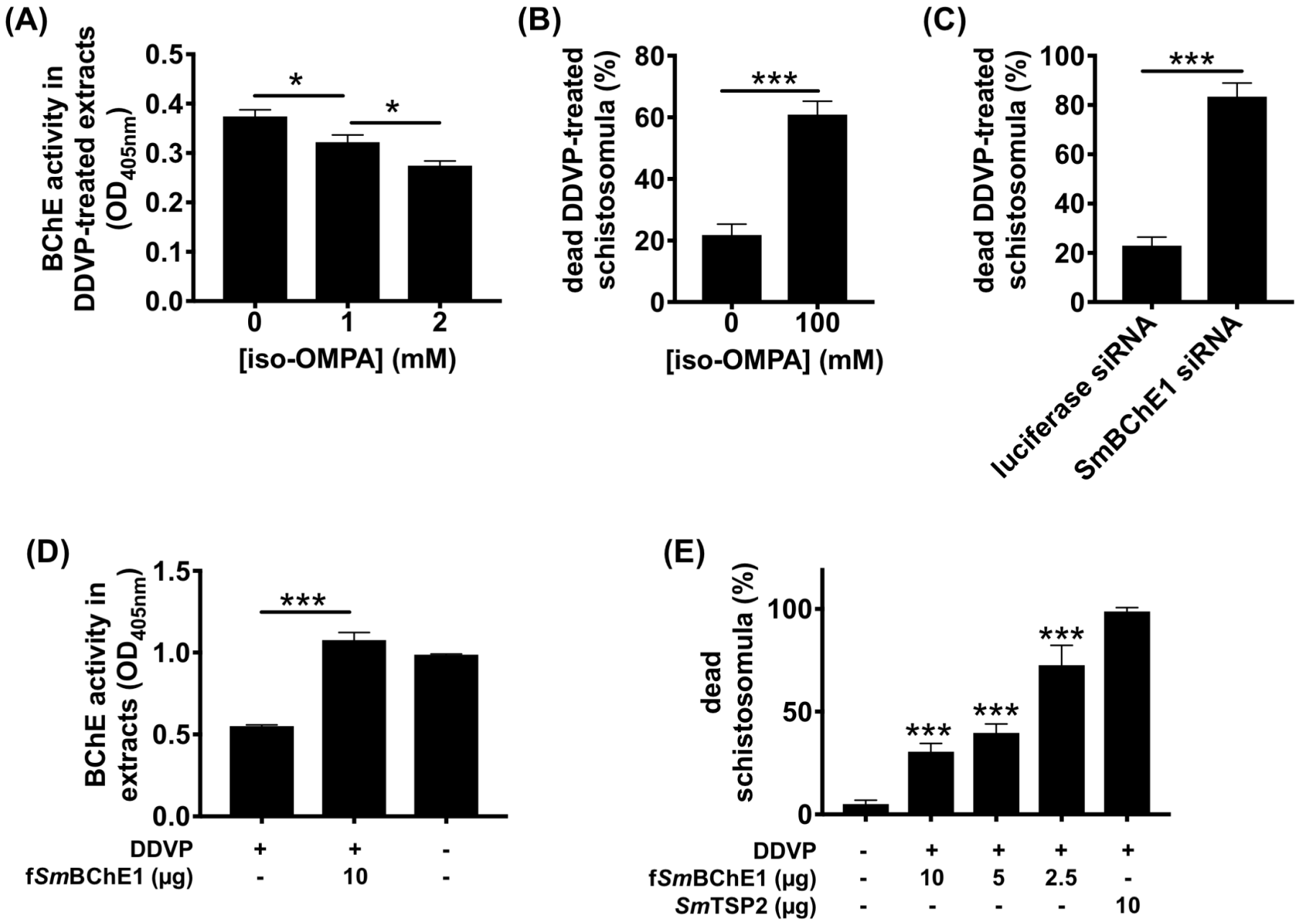

bioRxiv preprint doi: https://doi.org/10.1101/583658; this version posted March 21, 2019. The copyright holder for this preprint (which was not certified by peer review) is the author/funder, who has granted bioRxiv a license to display the preprint in perpetuity. It is made available under aCC-BY-NC-ND 4.0 International license.